

## Final Scientific Report for DOE/EERE

**Project Title:** “Low Cost, Epitaxial Growth of II-VI Materials for Multijunction Photovoltaic Cells”

**Covering Period:** September 1, 2011 to August 31, 2013

**Approved Project Period:** September 1, 2011 to January 31, 2014

**Submission Date:** April 30th, 2014

**Recipient:** PLANT PV  
5926 Ocean View Drive  
Oakland, CA 94618

**Website (if available)** [www.plantpv.com](http://www.plantpv.com)

**Award Number:** DE-EE0005332

**Working Partners:** The Molecular Foundry, Lawrence Berkeley National Lab

**Cost-Sharing Partners:**

**PI:** Brian Hardin  
Co-founder/President  
Phone: 650-814-0594  
Fax: 510-486-7424  
Email: [bhardin@plantpv.com](mailto:bhardin@plantpv.com)

**Submitted by:** Brian Hardin  
(if other than PI) Co-founder/President  
Phone: 650-814-0594  
Fax: 510-486-7424  
Email: [bhardin@plantpv.com](mailto:bhardin@plantpv.com)

**DOE Project Team:** DOE Contracting Officer – Jeannette Singen  
DOE Technical Project Officer – Daniel Stricker  
DOE Project Manager – Elaine Ulirch

---

Signature

Date

## Executive Summary

Multijunction solar cells have theoretical power conversion efficiencies in excess of 29% under one sun illumination and could become a highly disruptive technology if fabricated using low cost processing techniques to epitaxially grow defect tolerant, thin films on silicon. The PLANT PV/Molecular Foundry team studied the feasibility of using cadmium selenide (CdSe) as the wide band-gap, top cell and Si as the bottom cell in monolithically integrated tandem architecture. The greatest challenge in developing tandem solar cells is depositing wide band gap semiconductors that are both highly doped and have minority carrier lifetimes greater than 1 ns. The proposed research was to determine whether it is possible to rapidly grow CdSe films with sufficient minority carrier lifetimes and doping levels required to produce an open-circuit voltage (Voc) greater than 1.1V using close-space sublimation (CSS).

The two year research plan focused on 1) developing processing conditions to grow high quality CdSe on various types of substrates, 2) doping CdSe p-type, and 3) using advanced nanocharacterization techniques to examine how key morphological features (e.g. grain size, orientation, defect density, and strain) affect electronic materials properties such as the minority carrier lifetime. The expected outcome of the project was to develop a CdSe solar cell, grown on a silicon substrate, that is capable of producing an open-circuit voltage of >1.1V. Early modeling predicted that efficient devices would minimally require a doping density greater than  $>10^{16} \text{ cm}^{-3}$  and a minority carrier lifetime  $>1 \text{ ns}$  for the p-type CdSe layer. Our goal was to determine if these metrics could be achieved using the closed-space sublimation process. We designed a research program to develop processes to p- and n- type dope CdSe using the low-cost, high-rate CSS.

PLANT PV was able to successfully demonstrate p-type doping of CdSe to levels greater than  $10^{16} \text{ cm}^{-3}$  under CSS conditions. Several p-type doped CdSe films were confirmed by the National Institute of Standards. Previously, p-type doping of CdSe has only been demonstrated when using Molecular Beam Epitaxy, which is a slow growth, high cost method of deposition. PLANT PV also developed a confocal time-resolved photoluminescence decay measurement tool that is capable of measuring individual thin film grains in two-dimensions. Although a complete solar cell was not fabricated, all of the necessary thin film layers were deposited with sufficient electrical properties. The next phase will be to incorporate p-type doped CdSe layers into solar cells for device for testing.

With silicon based PV modules representing over 85% of the \$82 billion dollar annual solar power market, breakthroughs in the development of II-VI top cells can be integrated into existing manufacturing lines and have an immediate impact on the largest PV market segment. PLANT PV performed models and predicted that the addition of a CdSe top solar cell using closed-spaced sublimation could add less than  $\$30/\text{m}^2$  to existing Si manufacturing costs and boost power conversion efficiencies by >40%, allowing CdSe/Si tandems to meet the SunShot \$0.50/W goal. The understanding gained through the course of this research presents a viable path for a high-efficiency solar cell using the proposed CdSe/Si tandem architecture. We believe that this research demonstrates the feasibility of using CdSe grown via CSS as a wide band gap PV material.

## Comparison of Proposed versus Realized Project Goals

The following table summarizes the project’s proposed goals versus actual progress for each task. Deviations between an initial negotiated deliverables / milestones and an actual deliverable / milestone are discussed in the “Deliverable / Milestone Deviations” section of the Technical Narrative.

Task #	Task description	Initial Negotiated Deliverable / Milestone	Actual Deliverable / Milestone
1.1	Build and test close-spaced sublimation system	<ol style="list-style-type: none"> <li>1. Pump down to <math>10^{-6}</math> Torr</li> <li>2. &gt;1 deposition/hr</li> <li>3. Control and measure partial pressure of Ar, N<sub>2</sub>, O<sub>2</sub> to 1 mTorr accuracy</li> </ol>	<ol style="list-style-type: none"> <li>1. Initial Milestones 1,2,3 completed</li> <li>2. Additional chamber built with advanced capability:                             <ol style="list-style-type: none"> <li>a. Pump down to <math>10^{-8}</math> Torr</li> <li>b. &gt;4 deposition/hr</li> <li>c. Control and measure partial pressure of Ar, N<sub>2</sub>, O<sub>2</sub> to 1 mTorr accuracy</li> <li>d. in-situ RHEED</li> <li>e. Monatomic nitrogen plasma source</li> </ol> </li> </ol>
1.2	Deposit high quality CdSe on various single crystal substrates	<ol style="list-style-type: none"> <li>1. Deposit ~3<math>\mu</math>m thick films</li> <li>2. Achieve approximately 1:1 stoichiometry</li> <li>3. Achieve &lt;5 degrees grain misorientation over 100<math>\mu</math>m x 100<math>\mu</math>m area with etch pit density of &lt;10<sup>7</sup> cm<sup>2</sup></li> </ol>	<ol style="list-style-type: none"> <li>1. Initial Milestones 1,2,3 completed</li> <li>2. Deposited CdSe on sapphire and MBE grown single crystal ZnTe thin film on Si substrates and achieve highly oriented films as confirmed by EBSD and XRD</li> </ol>
1.3	n-type dope CdSe	<ol style="list-style-type: none"> <li>1. n-type doping of &gt;10<sup>17</sup> cm<sup>-3</sup></li> <li>2. Indium diffusional doping of 1-5x10<sup>17</sup> cm<sup>-3</sup></li> </ol>	<ol style="list-style-type: none"> <li>1. Initial Milestones 1 and 2 completed</li> </ol>

		into CdSe film	
1.4	p-type dope CdSe	<p>1. p-type doping of <math>&gt;10^{16} \text{ cm}^{-3}</math></p> <p>2. Nitrogen incorporation of <math>1-5 \times 10^{16} \text{ cm}^{-3}</math> into CdSe film</p>	<p>1. Initial Milestone 1 achieved (see below)</p> <p>2. Nitrogen incorporation milestone achieved as verified by SIMS</p> <p>3. Successfully doped CdZnTe to <math>1 \times 10^{17} \text{ cm}^{-3}</math> with a bandgap of approximately 1.8eV, which is sufficient for a highly efficient solar cell. CdZnTe is a surrogate for CdSe and allowed us to deposit doped ZnTe in a similar architecture to our final device</p> <p>4. Varied the doping density by changing the bandgap and the nitrogen flux.</p> <p>5. Deposited p-type doped CdSe with greater than <math>10 \times 10^{16} / \text{cm}^3</math> using CSS on intrinsic ZnTe on (211) and (100) oriented Silicon substrates using As-doped CdSe powder made from a boule provided by Pacific Northwest National Laboratory. Samples were verified at NIST.</p> <p>6. Deposited CdSe with atomic N flux in conjunction with Se overflux (<math>p \leq 10 \times 10^{15}</math>)</p> <p>7. Annealed CdSe:As boule samples in Cd overpressure at 500C</p>

			(level difficult to exactly determine but likely $p \leq 10e16$ )
2.1	Time-resolved photoluminescence of single crystal II-VI materials	<ol style="list-style-type: none"> <li>1. Build TRPL set-up with ability to measure lifetime of between 50ps-1<math>\mu</math>s</li> <li>2. Measure the minority carrier lifetime of single crystals of CdSe, ZnTe, and ZnSe that are 1 cm<sup>2</sup> (we anticipate the minority carrier lifetimes to be between 100ns-1<math>\mu</math>s)</li> <li>3. Measure the radiative recombination rate constant of single crystalline and polycrystalline CdSe films</li> </ol>	<ol style="list-style-type: none"> <li>1. Initial Milestone 1 achieved</li> <li>2. Developed an instrument that could measure 2D minority carrier lifetime map that could be referenced and overlaid on SEM image of II-VI film</li> <li>3. Performance limiting features (defects) isolated using optical and structural analysis</li> </ol>
2.2	Grain size versus minority carrier lifetime	<ol style="list-style-type: none"> <li>1. Create plot of minority carrier lifetime against average grain size</li> </ol>	<ol style="list-style-type: none"> <li>1. Initial Milestone 1 completed</li> <li>2. Two dimensional lifetime maps of CdSe crystals of varying sizes. However, this is no longer relevant since the films that are grown have highly oriented grains with very low angle grain boundaries.</li> <li>3. Investigation of highly oriented CdSe films with lower lifetimes compared to polycrystalline thin films</li> </ol>
2.3	Advanced characterization of CdSe films	<ol style="list-style-type: none"> <li>1. TEM images of four high quality CdSe samples (i.e. two lateral and two cross-sectional) and document the grain boundary angle for</li> </ol>	<ol style="list-style-type: none"> <li>1. PLANT PV has performed TEM of polycrystalline CdSe thin films grown on sapphire and ZnTe to study the origins of</li> </ol>

		<p>lateral sections and quantify the defect density for cross-sectioned samples</p> <p>2. Map the minority carrier lifetime of CdSe samples by perform TRPL with 400 nm resolution over 100 x 100µm area (we expect the minority carrier lifetime to be 10ns +/- 2 ns in regions away from grain boundaries)</p> <p>3. Map the photocurrent density of two CdSe solar cells with 50 nm resolution over 100 x 100µm area</p>	<p>defects.</p> <p>2. Demonstrated capability to map films and extract the lifetime at each point; created spatial maps of samples</p> <p>3. Oriented films that are grown on ZnTe (i.e., for solar cells) have no clear grain size making this task not as important as initially thought</p> <p>4. 2D TRPL map of discontinuous, polycrystalline CdSe thin film grown on sapphire measured a 7.6 ns lifetime!</p> <p>5. TRPL showed that polycrystalline films had longer lifetimes than “single crystal” films</p>
2.4	Device modeling	<p>1. Create a SCAPS model that describes the experimental JV behavior of CdSe PV devices in subtask 3.3</p> <p>2. Create an optical model describing optical losses and estimating the maximum achievable photocurrent density for CdSe PV device</p>	<p>1. Initial Milestone 1 and 2 not completed – no device therefore no device measurements to model</p> <p>2. Completed SCAPS modeling of thin film solar cells to understand the efficiency expected based on certain materials properties of the various layers of the solar cell (e.g., doping , defect density, etc.)</p> <p>3. Modeled the effects of the CdS window layer on device performance.</p>

3.1	Buffer incorporation layer	<p>1. Create ZnTe or ZnSe thin films with homogenous, lateral grain sizes of <math>&gt;20\mu\text{m}</math> confirmed by SEM and/or optical microscopy</p> <p>2. ZnTe or ZnSe thin films will be etched and examined in an SEM to verify an etch pit density <math>&lt;10^7 \text{ cm}^{-2}</math></p>	<p>1. We have doped the buffer layer (ZnTe) to levels needed so this task is complete.</p> <p>2. Also have grown p-type ZnTe on silicon using close-spaced sublimation so we can now grow CdSe films on single crystal and polycrystalline ZnTe.</p>
3.2	Fabrication of CdSe diode	<p>1. CdSe diode with shunt resistance greater than 300 ohms and a series resistance less than 20 ohms on a device area of <math>0.5 \text{ cm}^2</math></p>	<p>1. We made a heterojunction n-type CdSe/p+ ZnTe diode, which rectified.</p> <p>2. We have developed the ability to deposit a window layer (e.g., CdS or ZnSe) and TCO (e.g., ITO, AZO)</p> <p>3. We have made p+ Si/p+ ZnTe/p- CdZnTe/CdS/In diodes which rectified with good device characteristics.</p> <p>4. Good rectification has been achieved with a II-VI heterojunction on Si with relatively low contact resistance between ITO/II-VI (<math>45 \text{ m}\Omega\text{-cm}^2</math>).</p> <p>5. No homojunction diode made</p>
3.3	Fabrication of CdSe solar cell	<p>1. CdSe single junction PV device grown on silicon with a surface area <math>&gt;0.5 \text{ cm}^2</math>, an open-</p>	<p>1. We made an n-type CdSe/p+ ZnTe diode, which rectified.</p>

		circuit voltage >800 mV, EQE >70%, and a fill factor >0.70 under one sun illumination	2. We have made p <sup>+</sup> Si/p <sup>+</sup> ZnTe/p-CdZnTe/CdS/TO/In solar cells which rectified in the dark.
--	--	---	---

## Technical Narrative

### Project Objective

PLANT PV studied the feasibility of using CdSe to manufacture efficient (~25%) tandem solar cells that employ silicon and CdSe as the bottom and top solar cell materials, respectively. The two year research plan focused on 1) developing processing conditions to grow high quality CdSe on various single crystal substrates, 2) doping CdSe p-type, and 3) using advanced nanocharacterization techniques to examine how key morphological features (e.g. grain size, orientation, defect density, and strain) affect electronic materials properties such as the minority carrier lifetime. PLANT PV was able to demonstrate high p-type doping (i.e.  $>10^{16} \text{ cm}^{-3}$ ) of CdSe using closed-space sublimation (CSS) for the first time and were able to degenerately dope ZnTe under deposition rates of  $>1\mu\text{m}$ . These results are considered vital in proving the feasibility of making highly efficient CdSe solar cells.

Silicon based PV modules represent over 85% of the \$82 billion dollar annual solar power market. Si PV cell processing, packaging, and reliability are well established with a multitude of Si PV manufactures producing modules with power conversion efficiencies between 15-22% and standard lifetimes of 25 years. Silicon is a strong candidate for the bottom cell of a tandem device with a band gap of 1.1 eV and excellent PV properties. Furthermore, silicon wafers are one of the cheapest, most widely available single crystal substrates. Innovations in high Voc CdSe top cells can be rapidly integrated into existing Si PV manufacturing lines and have an immediate impact on the largest PV market segment. There is great opportunity to develop new module designs for CdSe/Si tandems based on Si substrate cost and efficiencies, which are described below, giving US manufactures opportunities to further differentiate their product while reducing costs to the \$0.50/W level. Finally, CdSe is known to be stable, which should not require drastic changes to packaging and encapsulation. We anticipate that 25 year lifetimes could be achieved for the CdSe/Si tandem system without substantial research efforts.

### Background

Multijunction solar cells that are composed of two solar cells have theoretical power conversion efficiencies in excess of 29% under one sun illumination and can become a highly disruptive technology by developing new architectures and processing techniques to significantly reduce production costs. The PLANT PV/Molecular Foundry team believes that one strategy to make low cost, highly efficient tandems is to grow high quality, defect tolerant, wide band gap thin films on silicon using closed-space sublimation. We proposed to study the feasibility of using cadmium selenide (CdSe) as the wide band-gap top cell and Si as the bottom cell in monolithically integrated tandem architecture. The greatest challenge in developing efficient tandem solar cells is achieving a high open circuit voltage (Voc) with the top cell. In the ideal case, 67% of the total power from a tandem solar cell comes from the wide band gap, top cell. In order to achieve tandem power conversion efficiencies greater than 25% the CdSe top cell must have a Voc greater than 1.1V. To date, only a small number of photovoltaic materials (e.g. GaAs, CdZnTe) fabricated with expensive deposition techniques have achieved an open-circuit voltage greater than 1V. As an example, CdZnTe grown using

Molecular Beam Epitaxy (MBE) produced a Voc of 1.34V. However, MBE is expensive (i.e. >\$2,000/m<sup>2</sup>) which limits current multijunction solar cells to high light concentration (>500x) applications, which adds significant complexity and great challenge to achieve the dollar-per-watt (\$1/W) initiative.

*The crucial question is whether or not it is possible to obtain a high Voc using lower-cost manufacturing techniques such as closed-space sublimation (CSS). It is possible to epitaxially grow thin films on crystalline substrates using CSS; however, the quality will invariably be lower and the defect density likely increased. Increased defect densities severely affect the performance of III-V materials making CSS a poor deposition choice. II-VI materials are believed to be more defect tolerant which may allow for comparably high Voc. The proposed research will determine whether it is possible to epitaxially grow CdSe films with sufficient minority carrier lifetimes (i.e. >3 ns) and p-type doping levels ( $10^{16}$  cm<sup>-3</sup>) required to produce an open-circuit voltage (Voc) greater than 1.1V using close-space sublimation (CSS).*

II-VI materials have a more ionic bonding character than III-V materials; the less directional, tight-binding nature of the electronic wavefunctions allows for greater screening in ionic materials making the trap states less localized in II-VI materials than III-V material systems. This difference allows II-VI materials to be more defect tolerant and could be fabricated with lower cost techniques compared with typical III-V processes. In fact, II-VI material systems have shown long minority carrier lifetimes in films with relatively high defect densities and quality epitaxial films have been grown on highly lattice mismatched Si substrates. Recent work by EPIR has shown that highly lattice mismatched (19.4%) CdZnTe epitaxially grown on Si produced a Voc of 1.34V, shown in figure 4.6 The power conversion efficiency of the single junction, CdZnTe device on Si was 16.4% with a Jsc of 16 mA/cm<sup>2</sup>, and FF of 0.77. However, the high efficiency device was not reproduced. This seminal work demonstrates that highly lattice mismatched II-VI materials are capable of producing high Voc required for tandems on Silicon substrates. However, this work was performed using MBE with an estimated production cost of \$2,000-5,000/m<sup>2</sup>. Our key addition to this area of research is to determine if CdSe, which has a lower lattice mismatch coefficient than CdZnTe, can achieve similar Voc (1.1-1.3V) and power conversion efficiencies using significantly cheaper fabrication equipment with higher throughput. Our approach has the potential to drop production costs by two orders of magnitude.

CdSe is a binary compound made from relatively abundant elements, has a moderate lattice mismatch (11.9%) with Si, and can be deposited using closed-space sublimation. CdSe is stable, highly absorptive with an ideal band gap ( $E_g = 1.72$  eV) for the top cell.<sup>25</sup> CdSe has an estimated raw material cost of only 0.02¢/W and can in principle meet the world's 17,000 TWhr demand. Yet with these seemingly good traits there are currently less than fifteen publications on the subject of thin film CdSe solar cells. CdSe solar cells have been almost exclusively fabricated on glass forming polycrystalline thin films with small grains. Ferekides et al. recently demonstrated a semi-transparent n-type CdSe solar cell grown on SnO<sub>2</sub> coated glass with a p-type ZnSe buffer layer with a short-circuit current density of >17 mA/cm<sup>2</sup> and a peak EQE of >90%. These devices had a near-infrared transmission of 80% demonstrating great potential to be used in four-terminal tandem devices. However the open circuit voltage was extremely low

(<500 mV) and is likely due to relatively small grains (<5 $\mu$ m) and poor electrical contacts. Only one study exists of epitaxially grown CdSe solar cells, Gashin et al. grew n-type CdSe on top of p-type ZnTe using evaporative deposition and achieved an open circuit voltage of 800mV and a power conversion efficiency of 6.7%. This Voc is considered to be close to the maximum potential Voc between p-ZnTe and n-CdSe without grading CdZnSe. There are no published studies on how CdSe morphology affects optoelectronic properties, which makes it extremely challenging to quantify the effects of surrounding layers, metal contacts, and doping density on device performance. Furthermore, there is only one published paper on p-type doping of CdSe by Yao et al which used MBE to nitrogen dope CdSe p-type to  $10^{17}$  cm<sup>-3</sup>. This proposal will attempt to answer several basic questions on how thin film morphology effects efficiency of CdSe devices.

## Significant Accomplishments

This project completed the primary task of proving the feasibility of using CdSe as an efficient tandem solar cell material. *The most significant achievement of this work was the p-type doping of CdSe using the low-cost, high deposition rate process of close-spaced sublimation (CSS).* The p-type doping of CdSe has never been demonstrated before using this process. *A second significant accomplishment is the demonstration of degenerate p-type doping of ZnTe using atomic nitrogen flux during CSS growth – a novel technique never before demonstrated under deposition rate conditions.* We have also developed an advanced characterization technique, 2D time-resolved photoluminescence, to probe the films we have deposited and investigate the link between morphology and electronic properties. Because we were only able to p-type dope CdSe very late in the program we were unable to fabricate a solar cell by the conclusion of this report.

PLANT PV believes that the key to develop low cost tandem solar cells is to study materials properties of wide band gap semiconductors grown using high deposition rate processes. The vast majority of tandem solar cell research has focused on using slow deposition rate (e.g. MOCVD and MBE) processes to grow single crystals to maximize PV cell efficiencies. While single crystal devices can be utilized for high concentration PV systems, where they typically represent only about 15% of the total system cost, they are prohibitively expensive for flat panel/low concentration systems.

During the Next Gen II program, PLANT PV was most interested in studying how key processing conditions such as deposition rate, chamber pressure, temperature, and spacing affect growth conditions of II-VI materials on silicon in order to determine if it was possible to cheaply grow thin films with properties that were good enough to make >15% efficient top cell solar cells (e.g. minority carrier lifetime >3 ns with p-type doping levels  $>10^{16} \text{ cm}^{-3}$ ). Over the course of the grant, PLANT PV built specialized chambers that could deposit II-VI materials over a wide range of conditions ranging from MBE to CSS on various single crystal substrates. We attempted to dope many different II-IV materials (e.g. CdSe, ZnTe, CdTe, CdZnTe, ZnSe) under various conditions and developed advanced nanocharacterization techniques to examine how key morphological features (e.g. grain size, orientation, defect density, and strain) affect electronic materials properties such as the minority carrier lifetime. To this end, we achieved this goal by completing all of the tasks associated with the layers for the final device. All subtasks in Task#1 were completed. Only a single subtask in Task#2 was not completed. However, the discovery that oriented films grown on ZnTe (i.e., for solar cells) have no clear grain size making but clearly low minority carrier lifetimes. During the course of our investigation determine that intragrain defects were largely responsible for low lifetimes. We expanded our capabilities to probe and quantify intragranular defects. The final task – CdSe device fabrication – was not completed. However, the all the components of the device were demonstrated and characterized. Several heterojunction diodes (i.e. p-ZnTe with n-CdSe) were fabricated and tested, but we did not have time to fabricate homojunction (p-CdSe with n-CdSe) devices prior to the writing of this report.

- Task#1 – CdSe Thin Film Deposition via Close-Spaced Sublimation
  - Built and qualified deposition systems
  - Deposited high-quality CdSe thin films on sapphire, and ZnTe substrates
  - Deposited n-type CdSe
  - Deposited p-type CdSe
- Task#2 – Advanced Characterization of CdSe Thin Films
  - TRPL measurements of II-VI single crystals
  - Define the relationship between CdSe grain size and minority carrier lifetime
  - Advanced characterization of CdSe thin films
  - CdSe device modeling
- Task#3 – CdSe PV Device Fabrication
  - Buffer layer incorporation
  - Fabrication of CdSe diode
  - Fabrication of CdSe-based solar cell

**Figure 1 shows the top level tasks and the supporting subtasks.**

The primary goals of this project are captured in our three primary tasks, which include: Task #1 – CdSe Thin Film Deposition via Closed-Space Sublimation; Task #2 – Advanced Characterization of CdSe Thin Films; and Task #3 – CdSe PV Device Fabrication. Figure 1 is included as a summary of the subtasks with check marks indicating completion. The accomplishments for each of the subtasks associated with these top-level will be discussed in detail below.

### **Task 1.1 Build and test close-spaced sublimation system:**

The first goal was to build a Closed-Space Sublimation (CSS) deposition system that could: a) provide a sufficient base pressure; b) provide a minimum of 1 deposition/hour; and c) control the pressure of processing gases to greater than 1 mTorr accuracy during deposition. Although CSS uses a high-pressure (typically > 1 mTorr) atmosphere for processing, we felt it was necessary to build a system that could be evacuated to the low-pressure regime ( $<10^{-6}$  Torr). This eliminated the contamination of growing films by background gases. Because the doping levels were very minute (ppm), any potential source of contamination needed to be controlled or eliminated. By the end of this phase, PLANT PV designed and constructed two close-spaced sublimation chambers (Figure 2), both of which are fully operational.

PLANT PV designed and constructed the first close-spaced sublimation chamber (Chamber #1), which was launched on December 15, 2011, approximately 45 days ahead of schedule. The chamber achieved a base pressure of  $10^{-6}$  Torr, independent source and substrate heating via halogen lamps, monitoring of the pressure, source and

substrate temperatures as well as the gas content of the atmosphere inside of the chamber during the deposition. The cycle time from sample loading to removal was approximately two hours with the chamber capable of handling a single substrate per deposition. The chamber was designed to allow PLANT PV to explore the processing conditions for close-spaced sublimation and is now being used for n-type doping experiments.

Chamber #2 is a more sophisticated system that was designed and constructed between Jan 15<sup>th</sup> and Mar 15<sup>th</sup> of 2012. The essential improvements over Chamber #1 are 1) the ability to load four substrates during one cycle, 2) automated control of source and substrate heaters, 3) lower base pressure ( $10^{-8}$  Torr) for a cleaner environment, 4) variable source/substrate spacing, 5) automated data logging and storage of all key processing parameters, 6) Reflection High Energy Electron Diffraction (RHEED) to examine quality of the substrates before deposition and 5) higher throughput (~2 samples/hr). The chamber has been used to deposit over 1200 CdSe films to date and has become the main CdSe deposition chamber for PLANT PV.



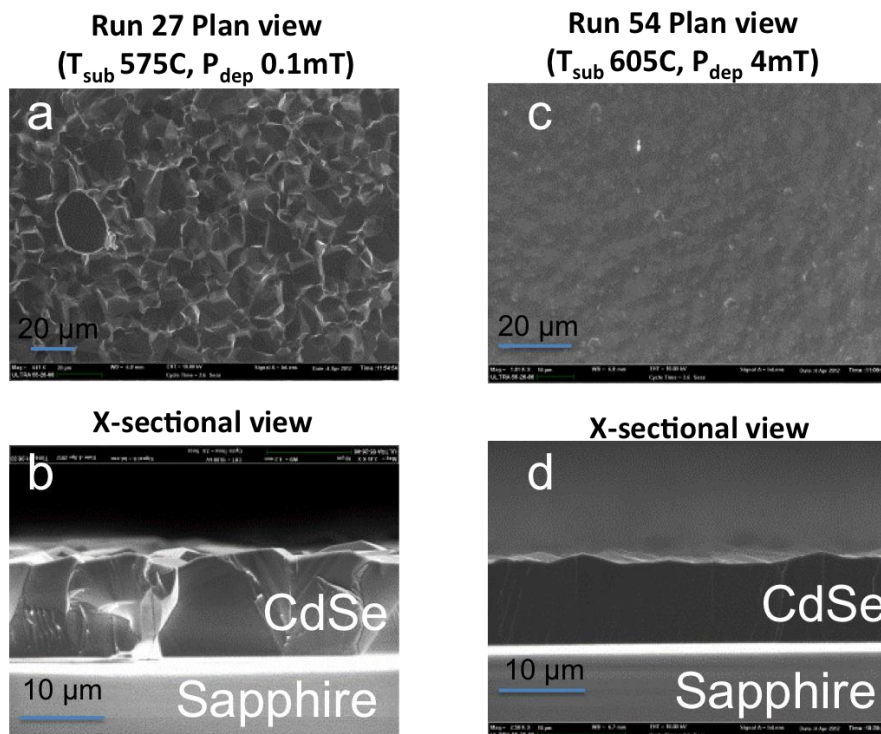
**Figure 2: Chambers 1 and 2 inside the cleanroom at the Molecular Foundry**

### **Task 1.2 Deposit high-quality CdSe on various single crystal substrates:**

Our next task was to demonstrate that the CSS process could be used effectively to deposit high-quality thin films on technical substrates. Many parameters affect film growth in close-spaced sublimation including the chamber pressure, substrate and source temperatures as well as the working distance between the substrate and source. All of these parameters can affect the film growth and quality. PLANT PV used combinatorial analysis by varying the growth conditions and analyzed the resulting films using SEM, XRD, and EBSD.

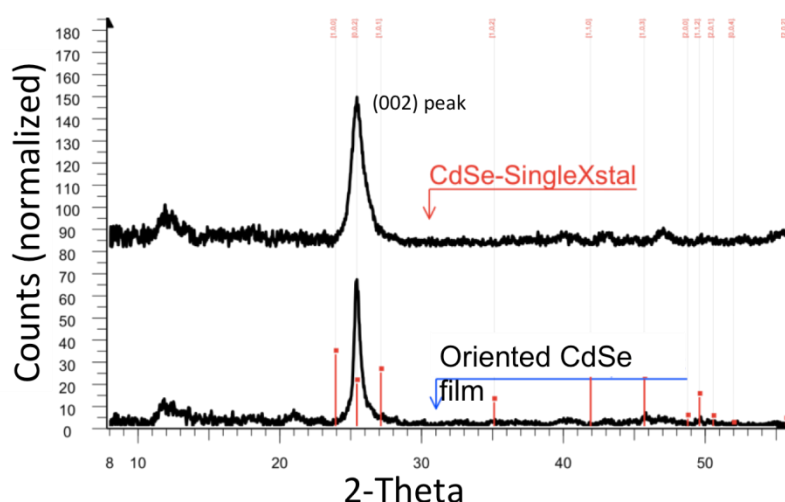
PLANT PV chose to study CdSe film growth on single crystal sapphire wafers as well as single crystal ZnTe grown on silicon wafers. Though CdSe has >10% lattice mismatch to sapphire, CdSe has previously been shown to grow epitaxially on sapphire making sapphire an easily procurable and thus excellent test substrate for film growth. The sapphire wafers were c-plane oriented and were purchased from a number of different vendors. ZnTe is approximately lattice matched to CdSe (~0.82%) and can also be grown epitaxially on silicon making ZnTe an excellent candidate as a buffer layer between CdSe and silicon for tandem solar cells. Single crystal ZnTe was grown for PLANT PV on (211) oriented silicon wafers by EPIR and on (100) oriented silicon by the Army Research Laboratory.

PLANT PV has deposited over 1200 films of CdSe on either sapphire or ZnTe substrates. Figure 3 shows SEM plan view and cross-sectional images of two different CdSe films (both in the wurtzite phase) grown on sapphire under different processing conditions but both at deposition rates of ~1 micron/minute. Figure 3a,b on the left shows a CdSe polycrystalline film with 5~30  $\mu\text{m}$  grains with visible grain boundaries both in the plan and cross-sectional views. Figure 3c,d shows images of a separate film of comparable thickness that was processed at a slightly higher temperature and pressure. Though the plan view shows a CdSe polycrystalline film with 3-15 micron grains, the cross-sectional view appears much more oriented with no apparent grain boundaries.



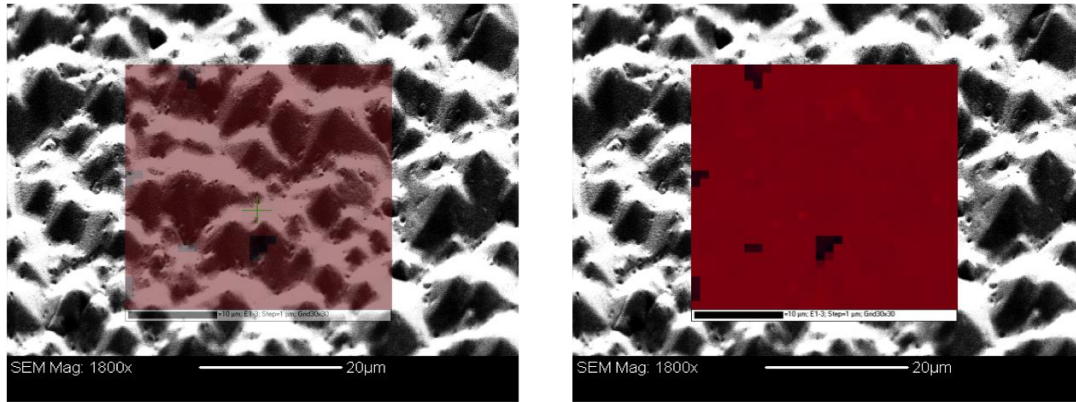
**Figure 3. Plan and cross-sectional SEM images of a randomly oriented polycrystalline CdSe film on sapphire (a,b) and a highly oriented polycrystalline**

To obtain a deeper understanding of the degree of orientation in our CdSe films on sapphire, grazing incidence x-ray diffraction was performed on various samples. Figure 4 is a theta/2-theta plot of an integrated cake segment of a CdSe single crystal purchased from MTI Inc and a highly oriented CdSe film grown at 1 micron/minute in PLANT PV's close-spaced sublimation chamber. Both films have the same orientation (c-plane oriented normal to the film surface) with no observable peaks from other lattice planes. This is a confirmation of the films having a high degree of orientation. However, the x-ray diffractometer at the Molecular Foundry used to perform x-ray diffraction is not well suited to detailed x-ray analysis, as it does not have a 5-axis goniometer. More detailed analysis, including pole figures and peak width characterization, requires a 5-axis goniometer, which was available to PLANT PV at the Stanford Synchrotron Light Source (SSRL).



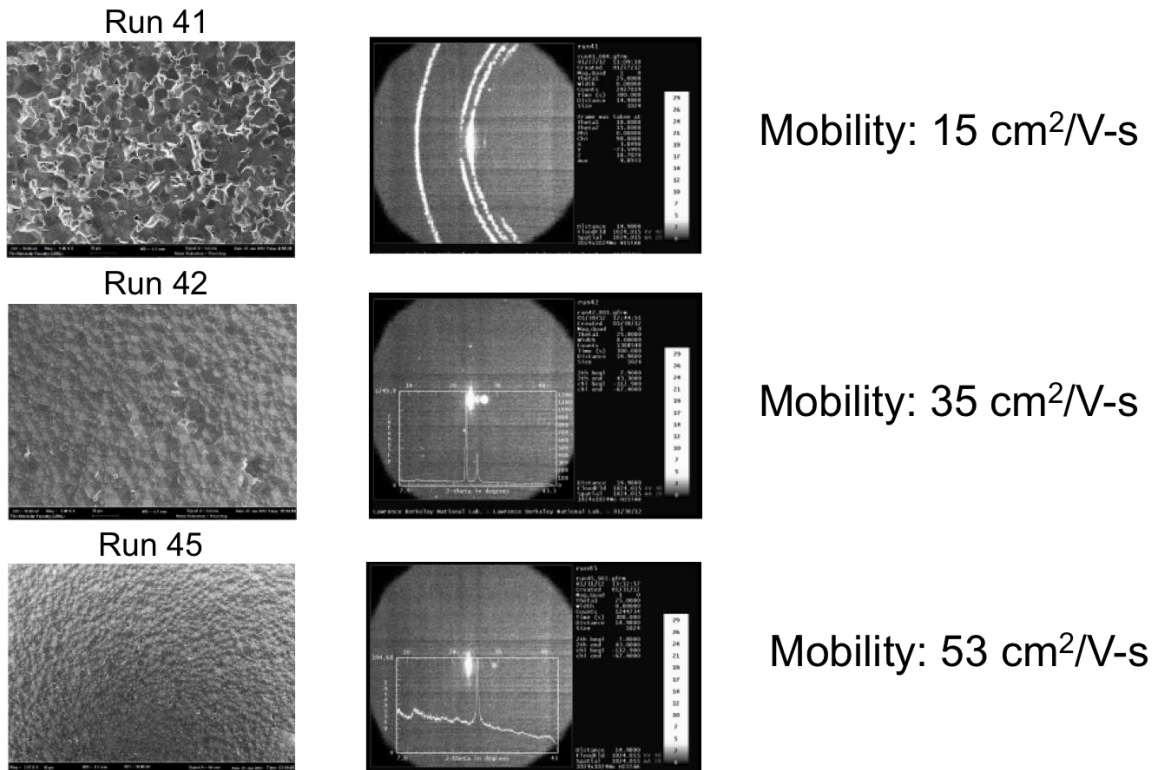
**Figure 4. Theta/2-theta plot from integrated cake segments of a CdSe single crystal highly oriented CdSe film on sapphire**

PLANT PV used electron backscatter diffraction (EBSD) to better understand the misorientation of small angle grain boundaries in the highly oriented CdSe films. EBSD was previously used by the multi-crystalline silicon solar community to characterize the types of grain boundaries present in their films and to better understand the effect of these different boundaries on electronic behavior. PLANT PV believes this same analysis will provide insight into the effect of small and large grain boundary angles in CdSe films. Figure 5 (left) shows an SEM image of an oriented CdSe film on sapphire with a semi-transparent overlay of an EBSD orientation map performed by PLANT PV. The misorientation between grains, calculated by differences in Euler angles, is seen more clearly on the right with the transparency set to zero. The analysis of the EBSD map in Figure 5 shows that with the exception of the darker shaded pixels, the misorientation in the entire region (~25x25 microns) is less than 2%. The darker shaded regions are small grains with larger misorientation, which can be >15%.



**Figure 5. SEM image of a CdSe film on sapphire with an overlay of the orientation (shaded region) measured by electron backscatter diffraction. The SEM image on the right is identical to the left with the exception that the shaded region is no longer transparent for easier viewing.**

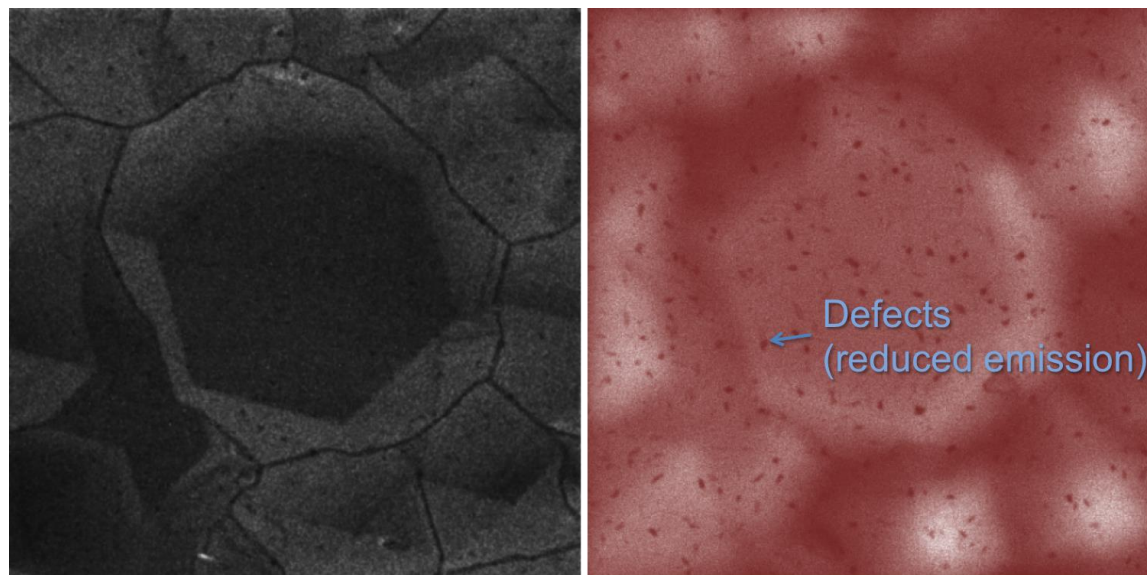
Finally, Hall measurements were made on CdSe films of varying degrees of orientation to better understand the in-plane charge carrier mobility as a function of film orientation. Figure 6 shows a series of films of increasing orientation along with the 2-dimensional detector images using grazing incidence x-ray diffraction and the resulting mobility using a Hall set-up. We observed an increase of almost 3x when going from polycrystalline to highly oriented films.



**Figure 6. Plan view SEM images (left), 2-d x-ray diffraction images (center) and charge carrier mobility (right) of three different CdSe films on sapphire of varying degrees of orientation.**

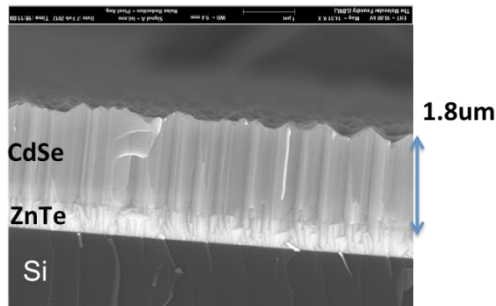
PLANT PV worked closely with Dr. Shaul Aloni at the Molecular Foundry to measure the defect density in the films using cathodoluminescence (CL) on various films. CL has previously been used by the research community to measure defects in thin semiconducting films and has certain advantages over etch pit density measurements. In particular, CL requires no etching of the film in order to perform measurements. While there are specific etching formulations for popular thin film materials (e.g. CdTe, ZnTe) there is no defined recipe for CdSe. CL operates by exciting charge carriers in the film through the use of an incident electron beam in an SEM chamber. Excited charge carriers can recombine radiatively and non-radiatively. Radiative recombination emits photons near the edge of the bandgap, which can be detected by using a fiber optic cable. By rastering the incident electron beam across the sample and observing differences in the contrast in luminescence, a map can be created showing dark spots or lines where luminescence-quenching sites exist in the film.

Figure 7 (left) shows a 10x10 micron plan view SEM image of CdSe on sapphire. The hexagonal structure is clearly visible in the large grain in the center. An overlay of the luminescence map obtained through CL measurements shows a number of dark spots that we believe are defects in the film. Though the SEM image on the left has dark specks, which are likely selenium deposits that occur at the end of the deposition, these do not correlate with the dark spots seen in the CL image on the right. Quantification of these defects leads to approximately  $10^8 \text{ cm}^{-2}$ . Further studies are now being performed on a number of films to correlate the film structure with defect type and density. At this stage we are still attempting to relate film processing and growth with different types of defects (e.g. point defects, defect loops, and holes).



**Figure 7: (Left) Plan view SEM image of CdSe on sapphire. (Right) CL map of defects (dark spots) in film. Figure dimensions are 10  $\mu\text{m}$  x 10  $\mu\text{m}$ .**

PLANT PV also grew CdSe films on single crystal ZnTe, which is in the zincblende (cubic) phase. The ZnTe layer (~1 micron thick) is undoped and was grown on (211) silicon by the Army Research Laboratory. We expected to grow highly oriented zincblende (cubic) CdSe films on ZnTe due to the small lattice mismatch between the two materials. Figure 8 shows a cross-sectional SEM image of a CdSe film grown by PLANT PV, which confirms that highly oriented CdSe will grow on ZnTe using close-spaced sublimation. Though the x-ray diffractometer at the Molecular Foundry is insufficient to confirm the crystal structure of the CdSe film, we believe it is the cubic phase. The CdSe film was grown at ~200 nm/min, which is slower than when grown on sapphire using similar processing conditions. This is likely due to the slower growth of the cubic phase relative to the hexagonal or the change in sticking coefficient between the source materials and the different substrates.



**Figure 8. Cross-sectional SEM image of a CdSe film grown on ZnTe/Si**

To better understand the relative orientation in the CdSe film between the grains, EBSD was used. Figure 9 (left image) shows a plan view SEM image of a highly oriented CdSe film on ZnTe. Clear structure is seen in this polycrystalline film. The blue line indicates a line scan across the sample using EBSD. The relative orientation (in degrees) can be seen on the plot to the right. A 35-micron distance shows on average <1-degree misorientation. It should be noted that the accuracy of the equipment is on the order of the misorientation seen in this scan (~0.5 degrees) so we can only conclude that these are very low angle grain boundaries.

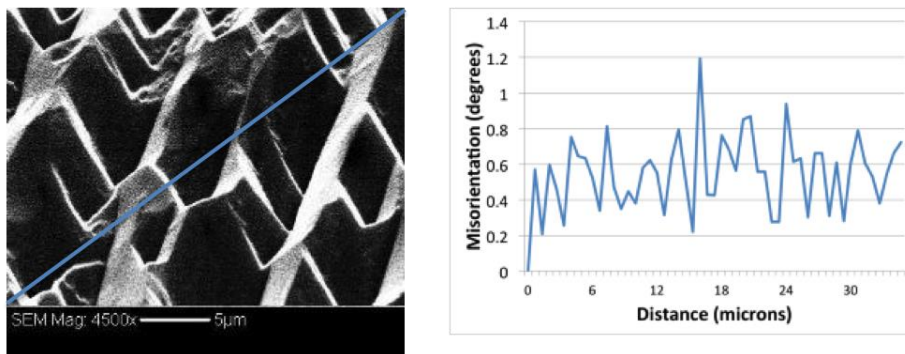


**Figure 9. (Left) Plan view SEM image of a CdSe film on ZnTe. The blue line indicates the direction and length of the line scan using EBSD. (Right) Relative misorientation (using Euler angles) of CdSe along line scan.**

PLANT PV was able to grow a large number of CdSe thin films with different morphologies depending on the substrate choice and processing conditions. In task 2 we describe how these morphologies affect the minority carrier lifetime of undoped CdSe thin films.

### **Task 1.3 n-type CdSe Doping**

PLANT PV has ex-situ and in-situ n-type doped CdSe using indium, which is a known n-type dopant. We ex-situ doped CdSe by evaporating a thin layer of indium onto the surface of a CdSe film followed by a rapid thermal annealing step to drive the indium into the film thickness. This enabled doping levels  $>10^{18} \text{ cm}^{-3}$ . However, this technique results in a non-uniform profile within the film without the formation of an abrupt junction.

PLANT PV then developed a method for in-situ doping during film deposition in the close-spaced sublimation chamber. The source powder was prepared by mixing CdSe powder together with a known quantity of indium selenide powder. The composite powder was then pressed and sintered in a metal die at high pressure to form a puck. The puck was then used as the source in the deposition chamber. Increasing or decreasing the amount of indium selenide powder in the puck controlled the level of indium doping. By doing this we were able to in-situ dope the CdSe film from  $10^{16}$  to  $10^{18} \text{ cm}^{-3}$ . EDX and XPS, which are both sensitive to about one atomic percent of the total composition, were used to confirm that no large deposits of indium were in the film. However, more sensitive analysis using secondary ion mass spectrometry (SIMS) was performed to understand the exact amount of indium incorporated into the films. SIMS analysis revealed uniform Indium doping in the deposited thin film as shown in Figure 10. We correlated SIMS data with our doping density measured via the Hall technique and found that indium activation was  $>90\%$ . We were able to n-type our CdSe to levels greater than  $>10^{18} \text{ cm}^{-3}$  via this technique. There was no additional heat treatment required to activate the Indium dopant. The ability to n-type CdSe without an activation step is significant since this reduces the required deposition steps for solar cell fabrication. The entire thin film can be deposited in-situ as an integrated step in the manufacturing process.

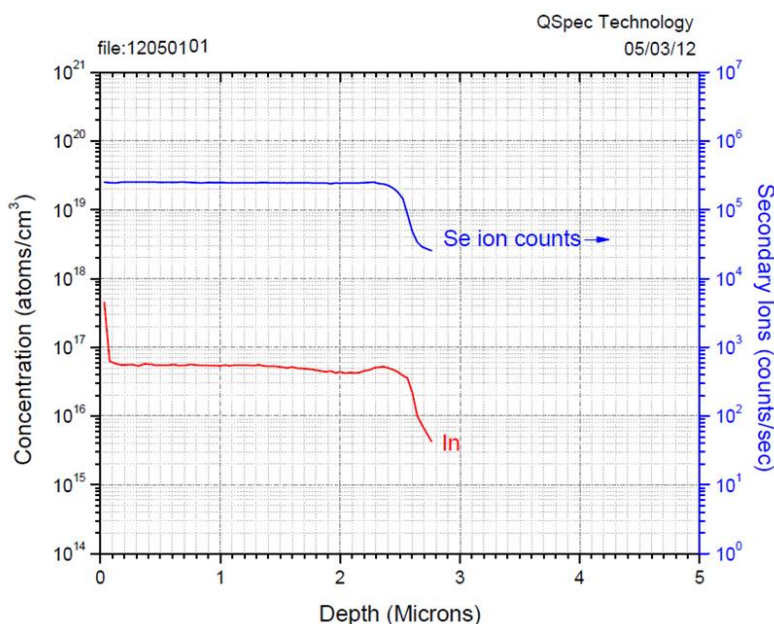


**Figure 10. SIMS profile of a CdSe:In film. The CdSe:In film was deposited using the CSS process in-situ. No additional heat treatment was required to activate the dopant.**

#### **Task 1.4 p-type CdSe Doping:**

The doping CdSe p-type was the most challenging task we attempted for the Next Gen II grant. The majority of PLANT PV effort was focused on solving this problem. Different pathways were explored throughout the duration of the program often in parallel with other efforts to accelerate the solution. To fully appreciate the scope of the effort, we discuss the work chronologically in this section.

##### *Initial Studies of CdSe p-type Doping (April 2012- January 2013)*

In the first 15 months of the grant period over 900 depositions of CdSe were performed. We were able to n-type dope CdSe using indium to our target levels relatively quickly in the project and switched quickly to work on the p-type doping problem.

Previously, Yao et al. (Applied Physics Letter 65, 466 (1994)) demonstrated 10<sup>17</sup> p-type doping of CdSe when grown via Molecular Beam Epitaxy (MBE) using a radical nitrogen source. These films were single crystalline and grown at a slow deposition rate. In the last twenty years no one has published a paper corroborating these results. There have also been no papers on p-type doping of CdSe using other impurities. However, there have been several papers published on p-type doping of CdTe and ZnTe that have provided impetus for our research (e.g. Baron et al. Journal of Crystal Growth 175, 682 (1997)).

We attempted to replicate certain aspects of the work in Yao's paper under slightly different conditions to dope CdSe using monatomic nitrogen on over 100 substrates. We were successful in p-type doping with nitrogen on five occasions but only to a maximum of 5\*10<sup>15</sup> cm<sup>-3</sup>. Over this period we varied the substrate type, growth rate,

substrate temperature, plasma power (and thus nitrogen flux) and chamber pressure (and thus mean free path). All of these attempts led to either intrinsic or n-type films with the exception of the five films previously mentioned. It should be noted that one of the films was verified to be p-type by the National Institute of Standards.

Two issues could cause low and inconsistent doping: nitrogen incorporation (i.e. not getting enough dopant gets into the film) or nitrogen activation (i.e. the nitrogen does not sit in the Se lattice site and affect the electronic properties or nitrogen forms a compensating defect with vacancies, oxygen, etc). We performed SIMS to measure nitrogen density in the CdSe thin films and determined that we could vary the nitrogen incorporation between  $10^{16}$  and  $10^{19}$   $\text{cm}^{-3}$ . A CdSe film with high nitrogen incorporation is shown in figure 11. Clearly nitrogen incorporation into CdSe, which achieved a density of  $10^{19}$   $\text{cm}^{-3}$ , was not an issue, but nitrogen activation proved to be extremely challenging. We worked with the Advanced Light Source to study dopant position in the CdSe lattice, but given the dopant type and concentrations it was very difficult to determine nitrogen position using x-ray absorption fine structure (XAFS) analysis.

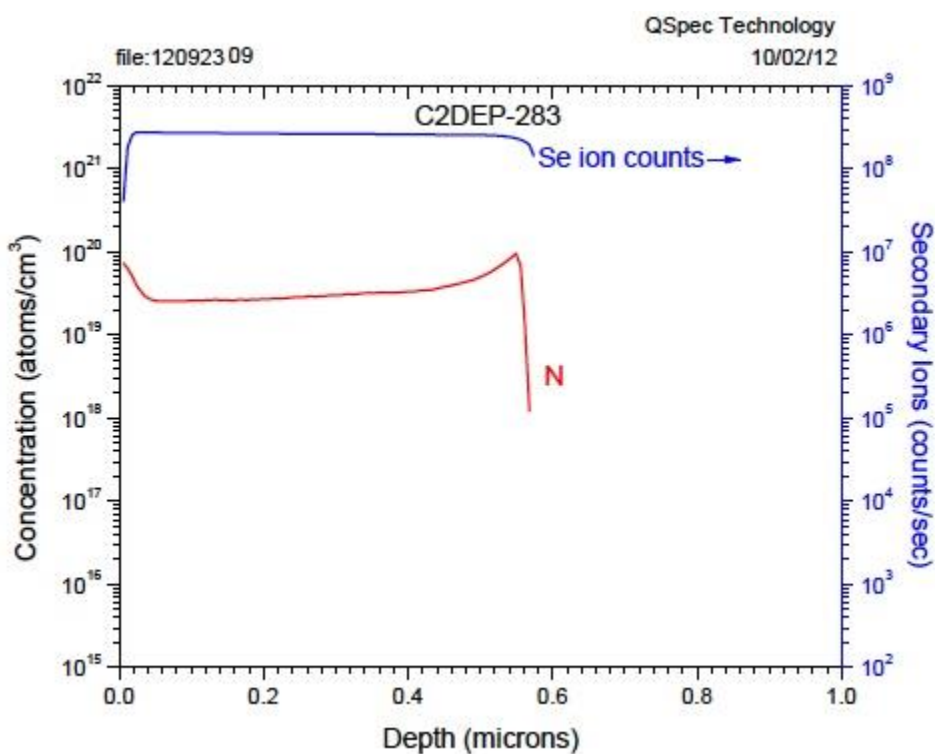


**Figure 11. SIMS profile of a CdSe:N film. Using radical nitrogen source we were able to incorporate  $>10^{19}$   $\text{cm}^{-3}$  nitrogen atoms into CdSe.**

In order to better understand nitrogen activation, we spent a lot of time analyzing the five p-type CdSe:N films to understand why they were doped. We performed x-ray fluorescence (XRF) spectroscopy at the Stanford Linear Accelerator (SLAC) to study impurity concentrations. The five p-type CdSe films were grown on a thin amorphous layer of ZnTe, which appeared to have diffused Zn into the CdSe film as evidenced by

XRF measurements. We thus began to suspect that the introduction of a second atomic species (e.g., Zn) as a co-dopant was important, which we will discuss later.

### *CdSe Doping Crossroads*

In late January of 2013 we formulated several questions regarding why CdSe was not easily doped p-type using nitrogen:

1. Can close-spaced sublimation conditions be used to nitrogen dope II-VI materials? Does high pressure CSS result in either a) unwanted inclusion of oxygen or hydrogen from the chamber, b) highly defective film structures that preclude activation, c) grain boundaries that result in dopant segregation (i.e. all of the nitrogen is near the grain boundaries and not in the bulk of the film), or d) deactivation of the monatomic nitrogen by other nitrogen species within CdSe films?
2. Is the plasma source generating the correct species of nitrogen for dopant incorporation and activation?
3. Do we need a co-dopant (e.g., Zn) in order to activate the nitrogen?
4. Is the stoichiometry of the CdSe film important for dopant incorporation and activation and do we thus need to have an overflux of one element (e.g., Cd, Se)?
5. Is the nitrogen going into the correct lattice site? How do we study this?
6. Is there another element that may also dope CdSe?

The first and second questions were critically important in evaluating our method for nitrogen doping. The logical next steps were to 1) begin using CSS and our plasma source to dope other II-VI materials that were well known to p-type dope using monatomic nitrogen and 2) begin to design and test a new source apparatus to enable multiple sources with independent control in order to study the effects of an overflux of a single element.

### *Attempts to dope other II-VI Materials*

The first question we wanted to solve was whether the lack of p-type doping was caused by the CSS processing conditions or was a problem that was specifically related to CdSe. ZnTe is known to be highly doped p-type by nitrogen in MBE and there were instances in the literature that it could be doped via sputter deposition.

It should be noted that doping ZnTe was a deliverable (Task 3.1) in our proposal since it would act as the buffer layer between the CdSe and silicon. ZnTe was also a logical choice because it only required one evaporator source. We were successfully able to degenerately dope polycrystalline ZnTe using our chamber (see discussion under Task 3.1), which led us to believe that problem with the nitrogen activation was related to the material properties of CdSe. ZnTe doping allowed us to calibrate the nitrogen flux from our plasma source. This result indicated that we are able to dope at least one II-VI material under CSS like conditions. This result is noteworthy and has not been previously demonstrated in literature. From this we discovered that the flux we were using to dope the CdSe films was extremely high, even at the lowest plasma power setting. We lowered the nitrogen flux by diluting the nitrogen with argon but had no success in doping CdSe p-type even by using a very low nitrogen flux.

Doping ZnTe was extremely useful because we 1) demonstrated that we could dope a II-VI materials under CSS conditions to high levels and 2) allowed us to meet our project management goal Task 3.1.

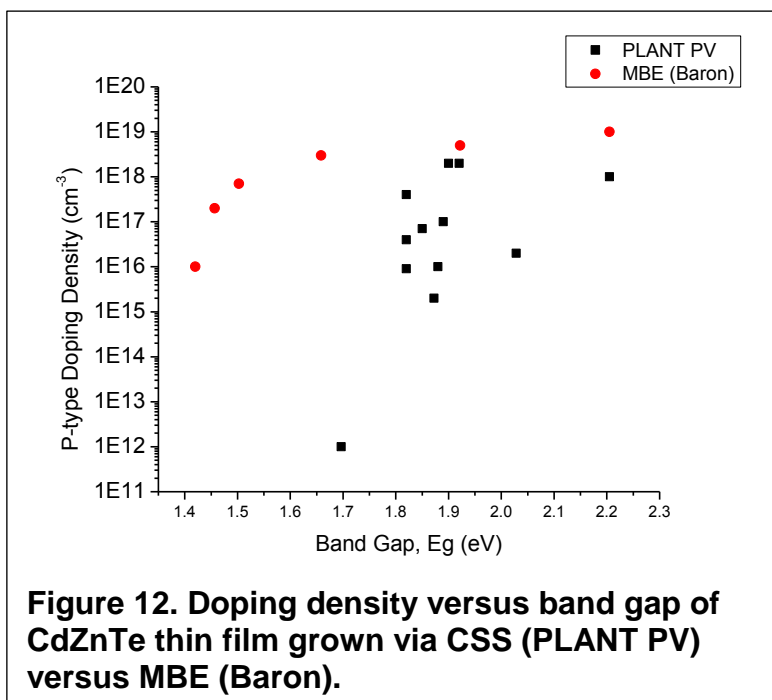
*Impact of Co-Doping: Using CdZnTe as a proxy for CdSe (April-May 2013)*

We also doped other II-VI materials that have been shown in the literature to be doped using nitrogen (e.g., CdZnTe) and added multiple sources to perform proper co-doping and single element overflux studies with CdSe. We retrofit chamber #2 to co-deposit from up to three sources and calibrated the positions to ensure uniform compositions over a 5 cm x 5 cm area. CdZnTe was an obvious material for us to choose since 1) we wanted experience in co-depositing II-VI materials and we already had experience depositing ZnTe, 2) it has been doped in the literature using monatomic nitrogen, 3) is well studied and thus our results could be compared with those in the literature and 4) has a relevant bandgap for a wide bandgap top solar cell and could thus be a potential candidate to make efficient tandem solar cells on silicon. Importantly, another intent was to eventually co-dope CdSe with Zn (in an attempt to replicate p-type CdSe films grown previously on amorphous Zn) and eventually to grow CdSe in a Cd rich environment. We did not perform these experiments first because it is exceptionally hard to measure the Cd flux in the chamber without sophisticated and expensive equipment and because we wanted to test Cd:Zn ratios in an analogous system with well-established results confirmed by multiple sources.

It took two months to retrofit our deposition chamber to allow for dual sources with independent controls. It should be noted that this was not a trivial task and required some time to design, build, install and test. We had to characterize the two sources independently and the uniformity of the resulting films as a function of distance and angular location from the source. We then optimized the geometry of the two sources to get consistent uniformity. One key observation was that the thermal drag from one source to the other source was too large to allow us to perform CdSe deposition studies with a Cd overflux, since Cd sublimates at relatively low temperatures (e.g., 170C). The thermal drag led to the minimum temperature on a source of 250C. This learning has fed into our thinking about a new design to controllably perform Cd overflux experiments, which we will discuss later.

As we planned the redesign to more easily thermally isolate the sources, we spent the rest of May and part of June co-depositing CdTe and ZnTe in order to understand how co-deposition depends on substrate temperature and starting powder amounts in each source. The sticking coefficients of each species are quite different at different substrate temperatures and we were able to properly learn and adjust processing conditions to account for this. As an example, the stoichiometry of a CdZnTe film changes from  $Cd_{0.4}Zn_{0.6}Te$  to  $Cd_{0.2}Zn_{0.8}Te$  when the substrate temperature goes from 400C to 500C, respectively. This has important implications for future overflux studies we perform using Cd with CdSe. We also did cross sectional EDX mapping of many films to ensure that the stoichiometry was consistent throughout the film, which is critical to achieving consistent results moving forward.

Figure 12 shows the p-type doping density versus the band gap of CdZnTe for CSS grown (PLANT PV) and MBE grown (Baron) thin films. By varying the Cd:Zn ratio it is possible to control the band gap of CdZnTe. We were able to successfully dope CdZnTe thin films with a band gap of  $\geq 1.8$  eV to greater than  $10^{16}$  cm<sup>-3</sup>, which is consistent with MBE grown thin films. For higher Cd loading (and lower band gap) CdZnTe thin films we found that the doping density would go down to levels that were significantly lower than CdZnTe films grown via MBE.



### *CdSe:N Overflux Study*

After demonstrating that we could successfully dope binary II-VI films (i.e. ZnTe) using a single source and dope ternary thin films (i.e. CdZnTe) using co-deposition we began to explore using Zn, Cd, and Se overfluxes to activate CdSe:N thin films. Previous work in the MBE community has suggested that an overpressure is required to ensure that the dopant goes into the correct lattice position (i.e. nitrogen in the Se lattice site). This can be accomplished by increasing the Cd overpressure of the system to generate Se vacancies.

We deposited CdSe using an overflux of Cd and found that there is a strong correlation between Cd overflux and doping levels. A high overflux of Cd results in n-type doping, regardless of whether or not we incorporate nitrogen into the films. Too low of a Cd flux leads to intrinsic films. Only on a handful of occasions did we achieve moderate p-type character with a moderate Cd overflux. During initial depositions, we were able to deposit films with reasonable ( $\sim 10^{14}$ ) p-type doping, but as the deposition experiments progressed, the films measured less and less p-type and trended to intrinsic (highly resistive) values. It likely that this is a result of the high vapor pressure and high mobility of pure Cd and Se substances in the chamber. Extensive cleaning would be necessary to restore the chamber to suitable conditions. Additional shielding should also be added to protect exposed surfaces in the chamber and reduce the contamination. Regardless, p-type doping using overfluxes were not reproducible and at this point we decided not to pursue nitrogen doping of CdSe.

### *Doping CdSe with Arsenic*

In the final months of the project we began exploring arsenic doping of CdSe in collaboration with Pacific Northwest National Laboratory (PNNL). P-type doping of CdTe thin films using arsenic has been previously shown in literature; however, no literature

exists on doping of CdSe with As. We received crystal boules of As-doped CdSe from PNNL that were first characterized with SIMS. CdSe boules had As concentrations between  $10^{17}$ - $10^{18}$   $\text{cm}^{-3}$ . We found that the single crystal pieces of CdSe:As to have either an intrinsic to slightly n-type character. It is common for II-VI single crystals to be grown under VI rich (i.e. Se or Te) conditions. For CdSe:As doped systems the excess Se could force the As into the Cd lattice, which would not result in p-type behavior.

We first attempted to activate the As by annealing CdSe:As single crystal pieces in a Cd overpressure for five days at 500C. Cd treated CdSe:As pieces exhibited a p-type doping of  $>10^{16}$   $\text{cm}^{-3}$ . Subsequent polishing of the surface that removed 100 um of the surface returned the boule to intrinsic character. Additional polishing had no effect on this behavior suggesting that the doping occurs in a thin layer of the material.

We then began growing CdSe:As thin films by grinding and then evaporating the doped boule in our CSS system. We found that depositing the CdSe:As powder onto ZnTe/Si substrates produced p-type CdSe thin films with doping densities greater than  $10^{16}$   $\text{cm}^{-3}$  as shown in table 1. This is a significant achievement because the thin film did not require a post treatment to activate the As dopant as we had previously hypothesized. All films to date that have been deposited on the ZnTe/Si substrates have been p-type with doping levels  $\geq 10^{16}$  concentrations. We measured the films in Table 1 using a commercially available Ecopia Hall measurement system at the Molecular Foundry. Our measurements show that both our CdSe and ZnTe are p-type with the values shown in Table 1.

PLANTPV has sent representative samples of p-type doped CdSe to the National Institute of Standards and Technology (NIST) for evaluation. Robert Thurber is a Hall measurement expert and previously evaluated our initial p-type doped CdSe thin films in a previous interim report. NIST performed hall measurement on a CdSe film (PLANT PV Sample: C2DEP1055) grown on ZnTe/Si and found comparable p-type doping levels to those found by PLANT PV, verifying our results. The confirmed results are available in the appendix A. Arsenic doped Cdse completed our quest to demonstrate that CSS can be used to fabricate all of the layers needed to build our envisioned tandem solar cell architecture. Unfortunately, these experiments were conducted in the last month of the project and have not yet been incorporated into devices (neither diodes nor solar cells) for further testing.

**Table 1. P-Type Doping Results of CdSe and ZnTe thin films**

Sample Number	Material	Film Thickness(um)	Substrate	Concentration	Resistivity	Mobility
820	ZnTe	1.3	Sapphire	2.48E+19	2.715	9.26E-02
821	ZnTe	2.5	Sapphire	1.31E+19	1.631	2.92E-01
822	ZnTe	7	Sapphire	1.53E+18	1.718	2.37E-01
1049	CdSe	2.3	ZnTe/(211)Si	1.59E+16	1.621	2.41E+02
<b>1055*</b>	<b>CdSe</b>	<b>7.3</b>	<b>ZnTe/(211)Si</b>	<b>2.47E+16</b>	<b>7.625</b>	<b>3.30E+01</b>
1057	CdSe	3	ZnTe/(211)Si	3.00E+16	1.62	1.25E+02

\* CdSe sample 1055 was sent to NIST, which confirmed that the p-type doping density was  $2.5 \times 10^{16}$   $\text{cm}^{-3}$ , which closely matches PLANT PV measurement. Faxed verification is provided in Appendix A.

It should be noted that polycrystalline CdSe thin films grown on sapphire did not exhibit the same p-type doping behavior as highly crystalline CdSe thin films grown on single crystal ZnTe/Si substrates. Unfortunately, we did not have time to study how morphological differences between CdSe films grown on sapphire versus ZnTe/Si could affect p-type doping, but feel that this is a fruitful area of research that could provide crucial information about the efficacy of doping more traditional, polycrystalline II-VI materials grown via CSS.

### Task 2.1 Time-resolved photoluminescence (TRPL) of single crystal II-VI materials:

PLANT PV constructed a TRPL tool at the Molecular Foundry that can measure the minority carrier lifetime of thin film semiconducting materials. The minority carrier lifetime is a direct gauge of the quality of a semiconducting material and will indicate whether or not a particular film is capable of producing a highly efficient solar cell. The key goal with using TRPL measurements was to understand the quality of our films without having to fabricate full solar cells, which can be time consuming, thereby dramatically speeding up the discovery process for high efficiency solar cells. The TRPL set-up is complete and fully operational and is briefly described below.

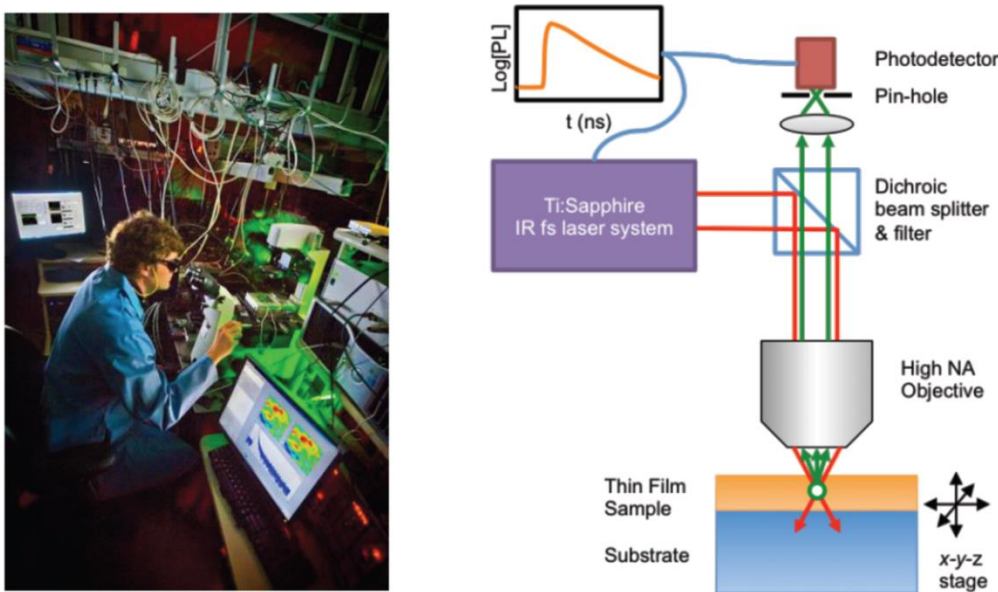


**Figure 12. A photograph of the actual TRPL instrument and an illustration of the instrument's key features.**

The TRPL set-up uses a femto-second pulsed laser with energy above the bandgap of the material of interest (e.g., CdSe). The pulsed laser is focused through an objective to achieve a spot size of  $\sim 1 \mu\text{m}$  and is absorbed by the thin film. Subsequent photoluminescence (PL) due to radiative recombination within the thin film is detected by an avalanche photodiode with a temporal resolution on the nanosecond timescale. The apparatus is depicted in Figure 12. The minority carrier lifetime can be extracted from the characteristic decay of the PL. However, care must be taken in extracting the lifetime from the PL decay curve as many competing processes are simultaneously

occurring within the bulk and at the surface of the films. In fact, a major problem with TRPL analysis is decoupling bulk recombination from surface recombination. Decoupling these two has become an important focus for PLANT PV.

We have built additional capabilities into the system that allow us to perform 2D time resolved TRPL mapping in order to evaluate the impact of grain size and substrate choice. We incorporated an x-y piezo stage, with 75 x 75  $\mu\text{m}$  mapping capabilities and 1 nm step precision, into the linear TRPL system. This allows us to study how the morphology affects the minority carrier lifetime and also to observe how homogenous the lifetime is in polycrystalline films. As an example, Figure 13 shows the TRPL map overlaid on the microscope image of a CdSe thin film.

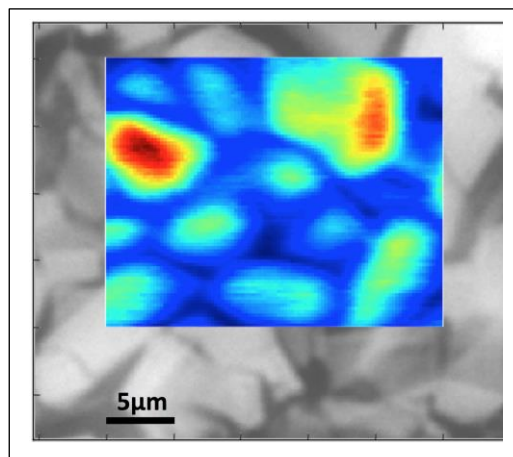


**Figure 13. Two-dimensional, linear TRPL map taken by PLANT PV/MF team of polycrystalline CdSe thin films overlaid above an optical micrograph. Scale is in microns. Red areas represent lifetimes of 5 ns while the blue regions represent lifetimes of 2 ns.**

We performed TRPL on both single crystal and polycrystalline CdSe, which will be presented below. Given the previous issues involving surface recombination we do not believe that it is possible to calculate the bulk radiation rate constant or achieve minority carrier lifetimes above  $>3$  ns for CdSe single crystals due to surface recombination effects. Because of these results we developed two-photon time resolved photoluminescence decay measurement system to reduce the influence the impact of surface recombination and published in Nature's Scientific Reports (doi: 10.1038/srep02098).

### **Task 2.2 Grain size versus minority carrier lifetime**

A large thrust of PLANT PV research was focused on growing high quality CdSe thin films and determining the key morphological parameters that affect the minority carrier lifetime of the CdSe thin films. We fabricated a wide array of CdSe thin films ranging from polycrystalline to quasi-single crystal on sapphire substrates. We also found that we were able to make highly oriented, quasi-single crystal CdSe thin films on epitaxially grown ZnTe on Si.

We previously hypothesized that growing the films with the largest grain size and highest orientation would result in films the highest minority carrier lifetime ( $\tau$ ). Therefore, we would expect that polycrystalline thin films would have the lowest minority carrier lifetime and quasi-single crystal films would provide the highest minority carrier lifetime. However, *initial work provided some surprising results: 2D TRPL mapping of polycrystalline CdSe films often resulted in an inhomogeneous distribution of lifetimes between grains with lifetimes ranging from 2-7ns. 2D TRPL mapping of quasi-single crystal CdSe thin films grown on ZnTe resulted in very uniform lifetimes of less than 1ns.*

In the most extreme example shown in Figure 14a, we grew a discontinuous, polycrystalline CdSe film that did not completely cover the sapphire substrate. We then performed 2D TRPL maps and found that some grains, shown in yellow, were much brighter than surrounding grains colored blue and pink. Several grains had minority carrier lifetimes of 7.6 ns (shown in figure 14b). These results indicate that individual grains of CdSe that are approximately 5 $\mu$ m in diameter may be sufficient for high efficiency CdSe solar cells. It should be noted that the initial PL decay of the long lived sample is not as drastic as for the polished single crystal CdSe sample shown in the previous report. While there is some surface recombination at the CdSe granular surface it does not appear to dominate the PL decay signal for this sample.

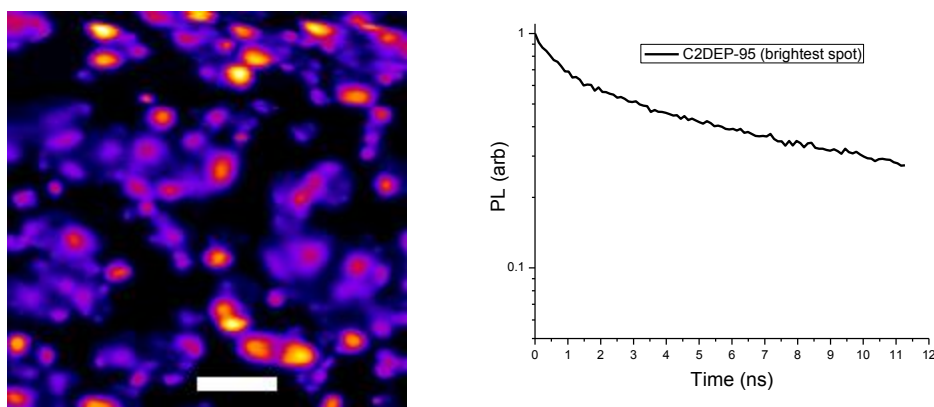


**Figure 14. (a) 2D TRPL map of a discontinuous, polycrystalline CdSe thin film grown on sapphire. The black portion is not photoluminescence (i.e. sapphire), bright grains with the longest lifetimes are colored in red and yellow and darker grains are colored in blue. The scale bar is 10 $\mu$ m. (b) Photoluminescence decay of individual CdSe grain with bright spot which has a 7.6ns lifetime.**

These results caused us to re-evaluate our original research thrust to study grain size versus minority carrier lifetime. We believe that the intragrain defect density of the polycrystalline CdSe films may be lower than the quasi-single crystal system. In polycrystalline systems, the defects can migrate to the grain boundaries, which can reduce the overall intragrain defect density. Quasi-single crystals may contain a higher density of intragrain defects due to the lack of grain boundaries. Given the low lattice mismatch between CdSe and ZnTe it is likely that we are experiencing epitaxial growth

during close-space sublimation and (threading dislocation) defects from ZnTe, which can be  $>10^8 \text{ cm}^{-2}$ , extend through the CdSe system.

Looking at this more closely, the bulk lifetime ( $\tau_{\text{bulk,eff}}$ ) is determined by the radiative ( $\tau_{\text{rad}}$ ), auger ( $\tau_{\text{Auger}}$ ), intragrain defect ( $\tau_{\text{bulk,eff}}$ ), and grain boundary ( $\tau_{\text{gb}}$ ) recombination processes, as shown in equation 1. The third term to the right hand side of the equation describes the intragrain defects and is modeled for a one-dimensional case. It can be seen that intragrain defect recombination depends on both the defect density ( $N_d$ ) and the charge carrier diffusivity ( $D$ ). Therefore lowering the defect density by 10x would increase the minority carrier lifetime by the same factor, assuming the minority carrier lifetime is predominantly limited by intragrain defects.

$$\frac{1}{\tau_{\text{bulk,eff}}} = \frac{1}{\tau_{\text{rad}}} + \frac{1}{\tau_{\text{Auger}}} + \frac{\pi^3 D N_d}{4} + \frac{1}{\tau_{\text{gb}}} \quad (\text{eqn. 1})$$

Figure 15 shows a plot of the effects of the intragrain defect density on the maximum minority carrier lifetime, assuming three different diffusivities. In this model we assumed that recombination was dominated by intragrain defects that were homogenously distributed in the film and that a defect was a perfect quenching site for minority carriers. As an example, for defect densities greater than  $10^8 \text{ cm}^{-2}$ , the minority carrier lifetime cannot be greater than 1ns for the expected diffusivity range of our CdSe thin films. Therefore,  $10^8 \text{ cm}^{-2}$  defect densities could be considered the lowest allowable defect density to produce efficient CdSe PV cells. It is extremely important that we are able to quantify the defect density and identify the origin of defects in both poly- and quasi-single crystal CdSe thin films.

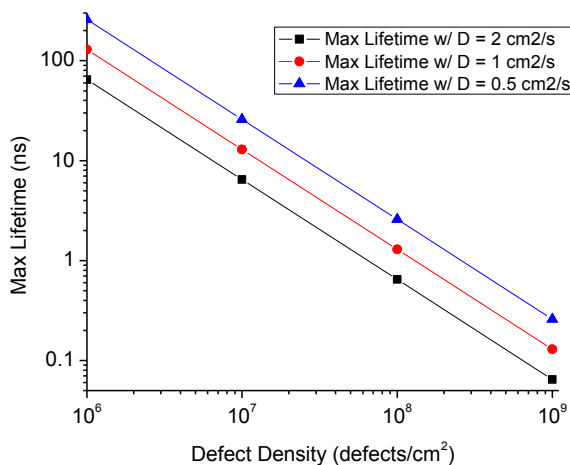


**Figure 15. Maximum minority carrier lifetime based on defect density ( $N_d$ ) and carrier diffusivity.**

### Task 2.3 Advanced characterization of CdSe films

We used several techniques to measure defects in CdSe thin films that are summarized

in the table below. Cathodoluminescence, etch pit density, and TEM all have some advantages and limitations that we briefly highlight below.

Technique	Measurable Defect Density Range
Cathodoluminescence	$10^3$ - $10^7$ $\text{cm}^{-2}$
TEM	$>10^7$ $\text{cm}^{-2}$
Etch Pit Density*	$10^3$ - $10^9$ $\text{cm}^{-2}$

To compare cathodoluminescence (CL) and etch pit density we studied several different ZnTe films that were epitaxially grown via MBE on (211) silicon by the Army Research Labs. One of the primary limitations of CL is that it cannot measure defect densities above  $10^8$   $\text{cm}^{-2}$  and cannot accurately quantify defect densities above  $10^7$   $\text{cm}^{-2}$ . Figure 16 is an SEM image (left) and CL image (right) of a defective ZnTe/Si sample. CL was performed at 10kV at 5,000x magnification; the CL image contains many blurred spots caused by the high defect density along with the extended electron bloom created by the 10kV electron beam and subsequent diffusion of excited minority carriers. Because we cannot resolve individual dark spots it is not possible estimate the defect density. It is preferable to use a lower electron beam voltage (e.g. 2-3 kV) but the photoluminescence quantum efficiency is low and the image quality is not improved.

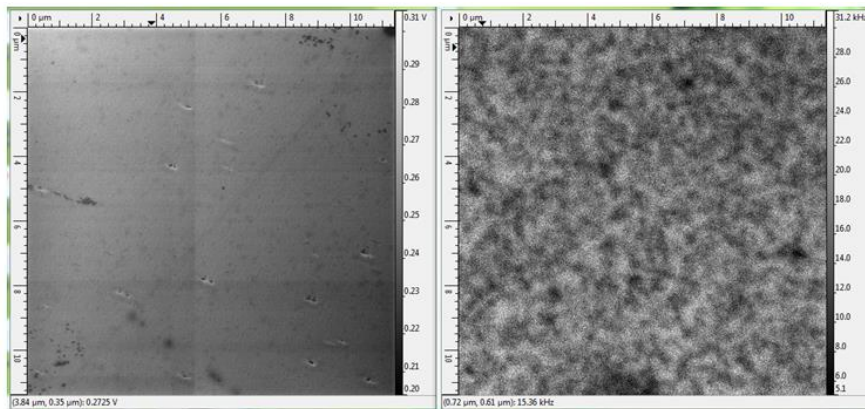


**Figure 16. (Left) SEM image (5kX magnification) of ZnTe grown on (211) silicon. (Right) CL image of ZnTe sample (same location and magnification) using 10kV electron beam. (Sample: ARL)**

It is possible to see individual defects when the density is below  $10^8$   $\text{cm}^{-2}$  as shown in the SEM (left)/CL(right) in Figure 17 below. The ZnTe/Si sample has fewer defects allowing us to image individual spots giving an estimated defect density of  $\sim 5 \cdot 10^7$   $\text{cm}^{-2}$ . Because the photoluminescence is higher it is possible to decrease the beam voltage, which improves the image resolution, while maintaining a high signal to noise ratio.

Calculated defect density between  $4.6\text{-}5.3 \times 10^7$  defects/cm<sup>2</sup>

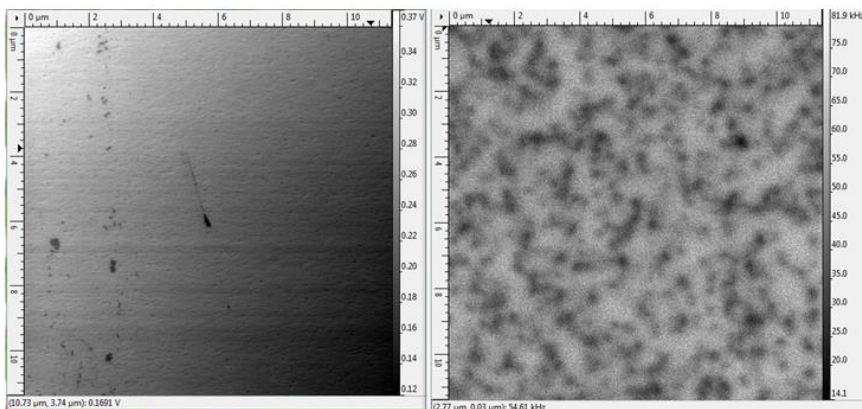


**Figure 17. (Left) SEM image (5kX magnification) of ZnTe grown on (211) silicon. (Right) CL image of ZnTe sample (same location and magnification) using 5kV electron beam. (Sample: ARL)**

Unlike CdSe, etch pit density (EPD) recipes of ZnTe are known. EPD process involves applying an etchant to expose the defects at the film surface and using SEM to measure individual pits. In Figure 18, we used a weak bromine etch to expose defects and found that the measured density was  $4 \times 10^8$  cm<sup>-2</sup>, which is an order of magnitude higher than the measured defect density using CL shown in figure 17. This result shows that cathodoluminescence does not provide an accurate measurement for high defect densities. The main limitation of EPD is that the technique requires a good etching recipe that specifically pits defects and crystal facets. Most of our films are fairly rough and have different exposed facets, which makes finding a good recipe challenging. We were not able to find an etching recipe that sharply pits CdSe well enough to take accurate EPD data.

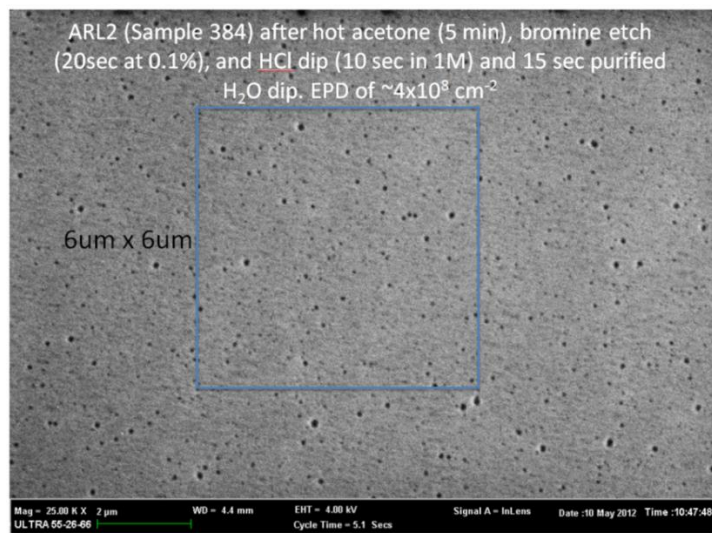


**Figure 18. SEM image (25kX magnification) of ZnTe after bromine etch. The defect density was calculated by measuring defects in a  $6\mu\text{m} \times 6\mu\text{m}$  box.**

TEM may be the most useful tool to both quantify high defect densities and determine their origin in CdSe thin films. We had a proposal accepted to study defects of CdSe films at the National Center for Electron Microscopy (NCEM) at Lawrence Berkeley National Labs. We worked at NCEM to quantify the defect density of the CdSe/ZnTe/Si samples and found that our films are highly defective for both polycrystalline CdSe (grown on Sapphire) and quasi-single crystalline CdSe grown on epitaxial ZnTe/Si substrates.

Figure 19 shows a micrograph of the interface between two grains of polycrystalline CdSe grown on sapphire. Here is seen a high angle grain boundary. Although the interface generates a large number of defects, one can see that the intragranular defects are lower than for the quasi-single crystal CdSe samples.

Arrows point in  $\langle 002 \rangle$   
Visible Angle between  
002 lattices: 20 degrees

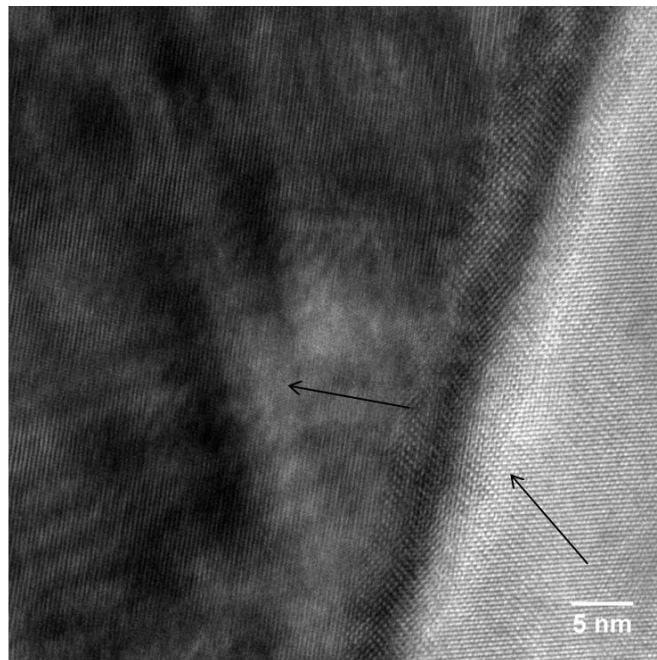


**Figure 19. A TEM micrograph showing the interface between two grains of polycrystalline CdSe that was grown on a (0001) sapphire. The arrows indicate the angle between the (002) planes for each grain.**

For quasi-single crystalline CdSe films grown on ZnTe/Si substrates, a different defect structure is observed. In Figure 20, we see the interface between the CdSe/ZnTe. There is a large number of defects generated at the interface and CdSe film (lower left portion of the micrograph) shows a large number of stacking faults. Although the lattice mismatch between the two materials is low ( $<1\%$ ), there are considerable defects generated at this interface. Looking further up into the film, we see that these defects propagate and also induce new defect structures like threading dislocations. Many of the ZnTe thin films used as substrates contained a high number of intragrain defects ( $>10^8 \text{ cm}^{-2}$ ), which can propagate through the CdSe during film growth. A high rate of defects can also occur in the CdSe due to the high deposition rate from the CSS process. The average defect density measured in these epitaxial films are  $>10^8 \text{ cm}^{-2}$

and are the primary reason why the minority carrier lifetime of “quasi-epitaxial” CdSe thin films have minority carrier lifetimes below 1 ns. Additional TEM images are available in Appendix B.

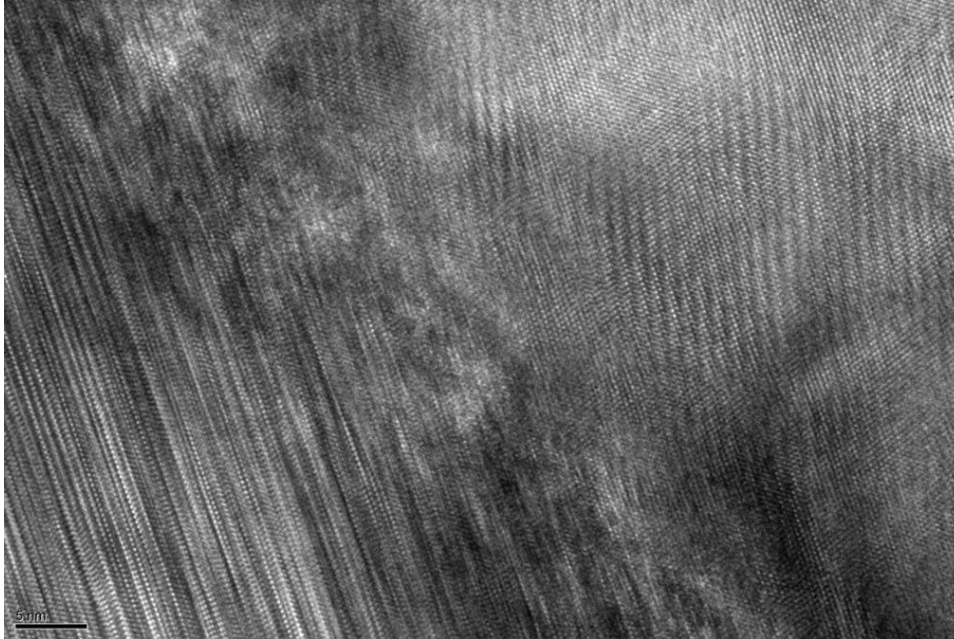


**Figure 20. A TEM micrograph of the interface between an epitaxially grown CdSe (bottom left) and a (211) ZnTe (top right) thin film on Si.**

#### **Task 2.4. Device Modeling:**

We have completed SCAPS modeling of thin film solar cells to understand the efficiency expected based on certain materials properties of the various layers of the solar cell (e.g., doping, defect density, etc.). We have also modeled the effects of the CdS window layer on device performance. We have included such results as our recent ZnTe and CdSe measured concentrations and defect densities in the modeling.

We have used SCAPS (a Solar Cell Capacitance Simulator) that is a 1D solar cell simulation tool designed out of Belgium (Department of Electronics and Information Systems (ELIS) of the University of Gent) for CIGS and CdTe devices – but very effective at modeling CdSe as well. The model can support up to seven semiconductor layers with grading and two contacts. The user can input different recombination mechanisms, which include band-to-band, Auger, and SRH. Defect types and profiles, bulk or interface and charge states and dopant distribution profiles can be input into the model. Contacts can be input as work function or flat band, along with their individual optical properties. Tunneling layers and/or phenomenon can be input as intra-band (e.g., within conduction band) or through interface states and users can define the generation profiles for excitation as well. Output from the model provides Dark IV, Light IV, EQE, CV, Cf profiles. SCAPS will also calculate bands and carrier profiles. Additionally, one can conduct batch processing by varying one or more parameters.

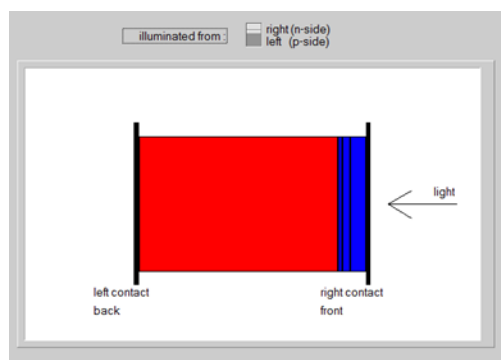


**Figure 21. An illustration of the architecture we used for our SCAPS modeling effort.**

We used the layer model shown in Figure 21 for our simulations using the solar cell architecture shown in figure 22. The SCAPS model included the tunnel junction and the homojunction for the p- and n-type CdSe layers.

We have modeled a CdSe homojunction solar cell using PC1D to better understand the key material requirements to make a 15% efficient top cell. We assumed a total device thickness of  $3\mu\text{m}$  with a 250nm n-type layer with a fixed doping density of  $10^{17}\text{cm}^{-3}$ . The electron and hole mobilities were assumed to be  $50\text{cm}^2/\text{Vs}$  and  $5\text{cm}^2/\text{Vs}$ , respectively, and the intrinsic carrier concentration of  $2.2 \times 10^5\text{cm}^{-3}$  was approximated using the density of states and the optical band gap. We assumed 10% reflectance off the front surface, front and rear surface recombination velocities of  $10^4\text{cm/s}$ , and additional materials parameters (e.g. index of refraction, dielectric constant, etc.) were taken from literature. The PC1D model should only be considered a rough guide since potential problems such as defect states at the CdSe/ZnTe interface were not included. By varying the materials parameters we found that the p-type doping density and minority carrier lifetime have the largest impact on efficiency, as shown in figure 22. For low doping densities (i.e.  $10^{14}\text{-}10^{15}\text{cm}^{-3}$ ) long lifetimes ( $\geq 100\text{ns}$ ) are required to produce devices with efficiencies  $>15\%$ . However, for highly p-type doped CdSe thin films a lifetime of 1 ns would result in a 16.7% efficient device with a  $V_{oc}$  of 1.03V,  $J_{sc}$  of  $20.2\text{mA/cm}^2$ , and a fill factor of 0.80. Though actual CdSe devices will likely have a larger series resistance and higher ideality factor, which will result in a lower FF, the  $V_{oc}$  estimates are fairly accurate. It should be noted that for minority carrier lifetimes greater than one nanosecond the internal quantum efficiency is relatively constant ( $<5\%$  change as the lifetime increases) at high doping levels, leading to a relatively constant short-circuit current density. The PC1D model results are similar to those obtained by others for CdTe devices and indicate that a lifetime of  $\geq 1\text{ns}$  with p-type doping of  $10^{17}\text{cm}^{-3}$  are sufficient for highly efficient CdSe devices.

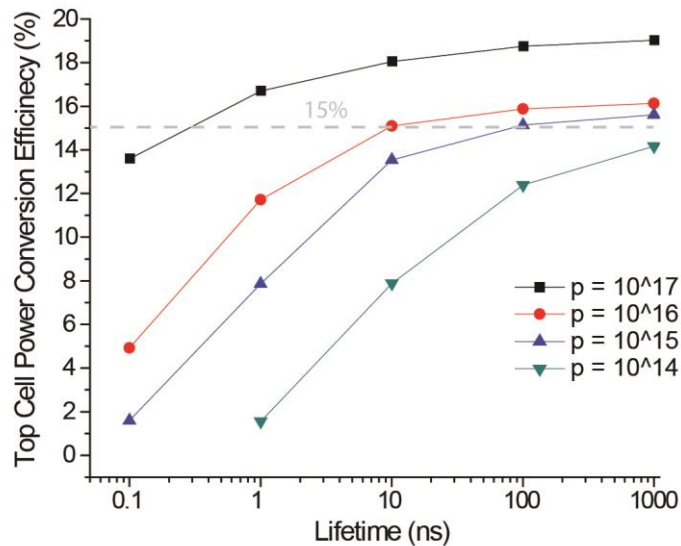


**Figure 22.** PC1D modeling of CdSe homojunction for various p-type doping densities and minority carrier lifetimes.

**Task 3.1 Buffer Layer Incorporation:**

This subtask involved depositing the non-photoactive layers (i.e. ZnTe, and ITO) needed to fabricate CdSe homojunction solar cells grown on degenerately doped silicon. The final CdSe/Si tandem architecture requires a tunnel junction composed of n<sup>+</sup>-Si and degenerately doped, p-type ZnTe, a CdSe homojunction, and a transparent conducting oxide layer (TCO), as shown in Figure 23. ZnTe was previously shown to be degenerately doped via MBE, but only achieved a doping density of 10<sup>17</sup> cm<sup>-3</sup> via sputtering. ZnTe must be doped to ≥10<sup>19</sup> cm<sup>-3</sup> in order to be an effective tunnel junction partner with n<sup>+</sup>-Si.

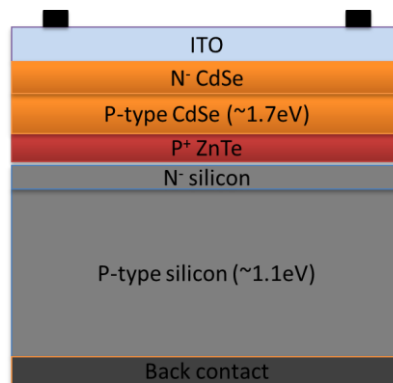


**Figure 23.** An illustration of our tandem solar cell architecture showing the additional layers required for fabrication of the complete device.

During the Next Gen II grant, PLANT PV developed techniques to degenerately dope polycrystalline ZnTe using radical nitrogen. The ZnTe doping levels of  $\geq 10^{19} \text{ cm}^{-3}$  were reproducibly attained at deposition rates of greater than  $1 \mu\text{m}/\text{min}$ . *Significantly, this is the first reported degenerate doping of polycrystalline ZnTe with atomic nitrogen and CSS.* This greatly enhanced our ability to construct the device with suitable electrical characteristics and improve Voc.

#### *Doping Polycrystalline ZnTe using a radical nitrogen source*

While attempting to dope CdSe under CSS conditions with a radical nitrogen source we began to experiment with p-type doping of ZnTe. PLANT PV was able to grow polycrystalline ZnTe films via close-spaced sublimation and doping levels approaching  $10^{20} \text{ cm}^{-3}$  have been achieved. Figure 24 (top) is a plan view SEM micrograph of a typical polycrystalline ZnTe film grown via CSS. Grain sizes can vary from 200nm to over  $1 \mu\text{m}$  through control of processing conditions. Figure 24 (bottom) is a plot of the doping density versus partial pressure of nitrogen in the chamber during growth of the ZnTe films. We are able to reproducibly control the doping levels of the ZnTe films from  $10^{13}$  to  $10^{20} \text{ cm}^{-3}$  by adjusting the flux of neutral nitrogen species on the surface of the film during growth. This level of doping in polycrystalline ZnTe films will allow PLANT PV to make a tunnel junction with the degenerately doped silicon substrate.

The ability to rapidly deposit degenerately doped ZnTe thin films has large ramifications for many types of tandem solar cells. While the quality and polycrystalline nature of the  $p^+$ -ZnTe thin films may not be suitable for traditional, single crystalline multijunction PV cells, it can be used for next generation multicrystalline systems. While CdSe/Si tandems are one route, ZnTe tunnel layer can also be used for CdZnTe/Si tandems and as the p-type layer for either single junction perovskites (in a substrate configuration) or with perovskite/Si based tandem architectures.

PLANT PV built a transparent conducting oxide, RF sputter chamber to deposit TCOs on CdSe. Indium tin oxide (ITO)

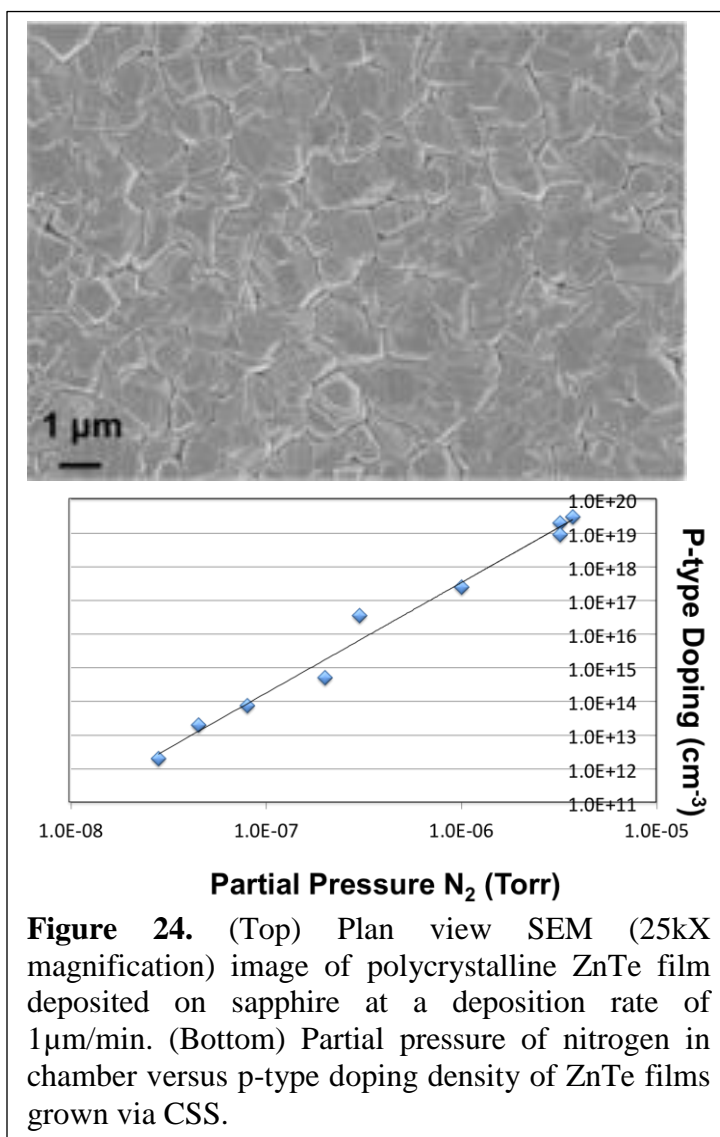


**Figure 24.** (Top) Plan view SEM (25kX magnification) image of polycrystalline ZnTe film deposited on sapphire at a deposition rate of  $1 \mu\text{m}/\text{min}$ . (Bottom) Partial pressure of nitrogen in chamber versus p-type doping density of ZnTe films grown via CSS.

serves as the top transparent conducting electrode. PLANT PV deposited ITO using a 3" diameter DC magnetron sputtering system. In order to achieve a 10% solar cell the ITO should have >80% transmissivity in the visible wavelengths with a sheet resistance of <30 ohms/sq. The top SEM cross-sectional SEM micrograph in figure 25 shows an ITO film sputter deposited by PLANT PV on a wide bandgap II-VI absorber. The bottom plot is of the transmission versus wavelength from 350-1200nm for a 250nm-thick ITO film on glass with a sheet resistance of 18 ohms/sq. Though further optimization would be needed to break 15%, we attained the properties required to fabricate a 10% efficient solar cell.

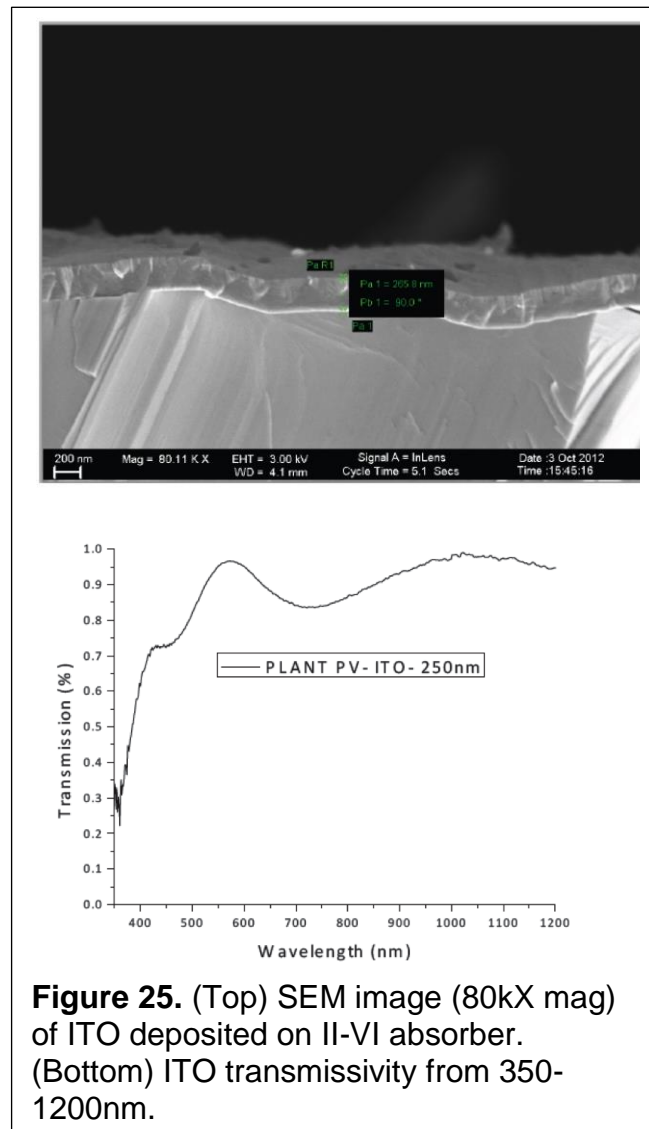


**Figure 25.** (Top) SEM image (80kX mag) of ITO deposited on II-VI absorber. (Bottom) ITO transmissivity from 350-1200nm.

### Task 3.2 Fabrication of CdSe diode:

Once the tunnel junction, n-type CdSe and window layers were qualified, we began fabricating devices to measure the electrical properties and optimize deposition

parameters. Although we did not have p-type CdSe for the final device, we deposited the n-type CdSe on p<sup>+</sup>-ZnTe/p<sup>+</sup>-Si substrates and added the ITO layer. The results of one such device is shown in Figure 26. The device exhibited a diode like behavior with rectification. The turn on voltage was at 0.7V. An SEM image of the interface between the n-type CdSe and the TCO layer (in this case ITO). Of note is the fact that the ITO forms a continuous layer on the CdSe film.

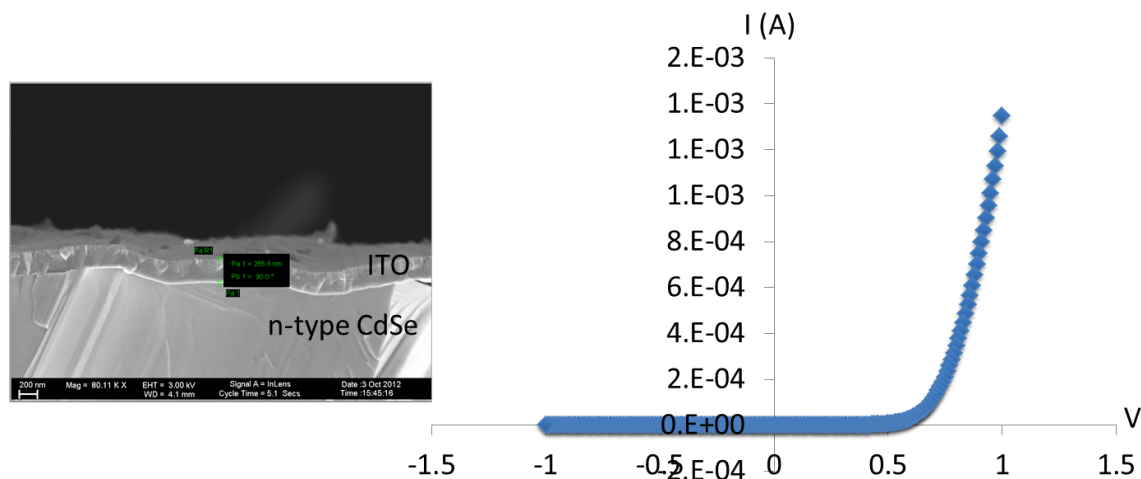


**Figure 26. A) graph of the I-V curve for an n-type CdSe/p<sup>+</sup> ZnTe diode showing rectifying behavior. The SEM micrograph to the left shows that the ITO is a continuous layer on the CdSe.**

### Task 3.3 Fabrication of CdSe Solar Cell:

This task was not completed. The primary reason was our successful p-type doping of CdSe was only realized in the final month of the program. The majority of our effort in the final six months was focused achieving high p-type doping levels of CdSe that would be required for high Voc solar cells.

### Important Questions/Areas of Research for future II-VI/Si Tandem Devices:

**II-VI Morphology Versus Lifetime:** Our work established that intragrain defects may be the dominant recombination mechanism for CSS grown CdSe thin films. One common question in the II-VI PV community is why polycrystalline thin films make better solar cells than single crystalline devices? Single crystal CdTe grown in ampoules often contain  $10^6 \text{ cm}^{-2}$  defects when grown with excess Te (and greater defect densities when grown with the correct stoichiometry). While it is possible to epitaxially growing II-VI thin films on lattice matched II-VI crystals these threading dislocations in the growth substrates typically propagate through the thin film and are not reduced unless grown over many microns. We found that intragrain defect densities were sufficiently high enough to be the dominant recombination mechanism in our “quasi-single” crystalline CdSe thin films. More in-depth studies could be performed to further determine how

overall grain size affects intragrain defect densities within polycrystalline CdTe and CdSe thin films using cathodoluminescence, 2D-TRPL, EBSD, and potentially TEM.

**As Doping of CdSe:** While we were successfully able to dope highly crystalline CdSe thin films p-type, we did not successfully dope polycrystalline CdSe (grown on sapphire) p-type over the last month of the project. Why “quasi-single” crystalline CdSe films are doped versus polycrystalline films is a critical question that could have wide spread impact in the II-VI community. CdSe:As could be used as a model system to explore the effects of grain boundaries and substrates on dopant incorporation and activation. SIMS, nano-auger, and/or atomic probe tomography could be used to determine the location and density of As in these films and XAFS could be used to determine if there are changes in the As position on the lattice. Increased doping of II-VI (i.e. CdTe) materials is a critical pathway to improve PV cell efficiency. A better understanding of the role of grain boundaries and other morphological factors on doping is crucial to making highly efficient II-VI solar cells in the future.

**Combining As Doping with high minority carrier lifetimes:** We demonstrated minority carrier lifetimes over 7 ns for discontinuous CdSe films and 5 ns with continuous polycrystalline CdSe thin films. All films where minority carrier lifetime data was presented were undoped. It is necessary to produce >1 ns lifetime with  $\geq 10^{17} \text{ cm}^{-3}$  p-type doping levels to make CdSe solar cells a feasible alternative. Further research is required to determine if As doping to  $>10^{16} \text{ cm}^{-3}$  levels affects the minority carrier lifetime.

**Making single junction CdSe solar cells on silicon:** While PLANT PV was able to demonstrate new methods to dope CdSe and ZnTe we did not have time to complete PV cells during this grant. This report lays the ground work to both dope and grow CdSe and ZnTe on silicon. It is now possible to fabricate complete CdSe homojunction devices and fully explore the effects of morphology, doping, and lifetime on PV cell efficiencies.

### **Deliverable / Milestone Deviations**

The following Deliverable / Milestone deviations were conducted throughout the course of this investigation. Each deviation is matched to the task and subtask of the initial negotiated deliverables. In each case, the project manager approved the deviations after discussion and deliberation. All deviations were conducted to further the primary goals of the project.

#### **Task 1.1 - Build and test close-spaced sublimation system:**

This task was modified. Instead of a single deposition chamber, PLANT PV built one additional, more advanced close-spaced sublimation chambers in Q4 2011-Q1 2012 to deposit II-VI materials. We put substantial effort into building out and testing both chambers by depositing CdSe films. The advanced chamber allows for accurate control of the source and substrate temperatures, the source/substrate separation, the pressure and the monatomic nitrogen flux. This is a single source design so that CdSe powder could be sublimated and condensed onto a substrate. The chamber is also equipped with an automated shutter to accurately control the exposure of the substrate to the source.

#### **Task 1.4 - p-type Doping of CdSe:**

This task was amended to include CdZnTe. We studied p-type doping of CdZnTe in order to optimize doping conditions for CdSe. CdZnTe is a wide bandgap material that can be used for the tandem solar cell. We successfully doped CdZnTe to  $10^{17} \text{ cm}^{-3}$  with a bandgap of approximately 1.8eV, which is sufficient for a highly efficient solar cell. We were also able to vary the doping density by changing the bandgap (composition) and the nitrogen flux. Late in the project timeline, we successfully grew p-type doped CdSe with greater than  $10^{16} \text{ cm}^{-3}$  using the CSS process on intrinsic ZnTe on (211) and (100) oriented Silicon substrates. To achieve this, we used As-doped CdSe powder made from a boule provided by Pacific Northwest National Laboratory. The provided CdSe boule was doped to  $\sim 2 \times 10^{17} / \text{cm}^{-3}$  arsenic. The dopant level and carrier type were then independently verified at NIST. Additionally, we were able to deposit CdSe with atomic N flux in conjunction with Se overflux, but at insufficient levels ( $p \leq 10^{15} \text{ cm}^{-3}$ ).

#### **Task 2.1 – Time-resolved Photoluminescence of Single Crystal II-VI Materials:**

This task was modified. In addition to the instrument itself, we incorporated the capability to scan in two-dimensions.

#### **Task 2.2 – Grain Size versus Minority Carrier Lifetime:**

This task was modified. Deposited thin films of CdSe on final device layers like ZnTe were epitaxial. This fact eliminated the need to investigate the grain size versus minority carrier lifetime. Instead, we focused on looking at the intragranular structure with our 2D capability. Later, we looked at large grain structures deposited on sapphire substrates.

### **Task 2.3 – Advanced Characterization of CdSe Films:**

This task was modified. In addition to what has been shown, we have spent a lot of time developing capabilities to perform advanced characterization on thin film materials including: Two-photon PL & TRPL (2D and 3D mapping); Low temperature PL; Electron backscatter diffraction; CV, DLCP, 4-point probe; EXAFS, NEXAFS. In addition, we had proposals accepted at SSRL and NCEM. Both of these allowed us time for highly specialized structural and chemical investigation of our thin films and source materials.

### **Task 2.4 – Device Modeling:**

This task was modified. We completed SCAPS modeling of thin film solar cells to understand the efficiency expected based on certain materials properties of the various layers of the solar cell (e.g., doping, defect density, etc.). We also modeled the effects of the CdS window layer on device performance. However, we did not make a p-type CdSe solar and did not collect measurements; therefore, we did not model the device and compare the experimental values with those of the model as originally planned. We have included the results of our recent ZnTe and CdSe measured concentrations in the modeling.

### **Task 3.1 – Buffer Layer Incorporation:**

This task was modified. We doped the buffer layer (ZnTe) to levels needed so this task was completed. In addition, we also have grown p-type ZnTe on silicon using close-spaced sublimation so we can now grow CdSe films on single crystal and polycrystalline ZnTe. We verified our measurements on local equipment and sent samples to NIST where they were verified for doping concentration and doping character.

### **Task 3.2 – Fabrication of CdSe Diode:**

This task was modified. We made a heterojunction n-type CdSe/p+ ZnTe diode, which rectified. We also developed the ability to deposit a window layer (e.g., CdS or ZnSe) and TCO (e.g., ITO, AZO). We have made p+ Si/p+ ZnTe/p-CdZnTe/CdS/In diodes which rectified with good device characteristics. Good rectification has been achieved with a II-VI heterojunction on Si with relatively low contact resistance between ITO/II-VI (45 mW-cm<sup>2</sup>). No homojunction diode was made.

### **Task 3.3 – Fabrication of CdSe Solar Cell:**

This task was modified. We made p+ Si/p+ ZnTe/p-CdZnTe/CdS/TO/In solar cells which rectified in the dark. We are now working to make a full CdSe solar cell. We did not fabricate a CdSe homojunction device.

**Conclusion:**

PLANT PV has consistently gone above and beyond the effort that was negotiated in our original contract with the DOE. We raised private capital and spent approximately 50% more research hours on this project above the negotiated 20% cost share. We focused our research efforts on achieving minority carrier lifetime and p-type doping to levels that are required to make good solar cells. Our philosophy for the NextGen II grant was to determine if it was possible to achieve minority carrier lifetimes greater than 1ns and p-type doping of CdSe greater than  $10^{16} \text{ cm}^{-3}$ . We achieved these goals and believe that CdSe solar cells could achieve power conversion efficiencies of >15% when grown on silicon and that CdSe/Si tandems could achieve overall power conversion efficiencies of >25%. Future effort will be needed to ensure that high lifetimes can be achieved with high doping levels when grown on Si, but the results of the Next Gen II study are extremely promising.

## Outputs Developed Under the Award

### Patents / Licensing Agreements

Multi-crystalline II-VI based Multijunction Solar Cells and Modules Application No. 13/750,756

P-type doping II-VI materials under high pressure, high deposition rate with rapid thermal deposition using radical nitrogen (Provisional Application #: 16664740)

### Honors and/or Awards

None

### Publications

Barnard et al. Probing carrier lifetimes in photovoltaic materials using subsurface two-photon microscopy, Scientific Reports vol 3 2098 (2013)

### Presentations

Dr. Brian Hardin\*, Dr. Edward Barnard, Dr. James Groves, Dr. Stephen Connor, Dr. Craig Peters, "Life After Graduate School", Energy Frontier Research Center Workshop, Stanford Linear Accelerator (SLAC), Stanford, CA, 4/13/2012

Dr. Edward Barnard\*, Dr. Brian Hardin, Dr. James Groves, Dr. Stephen Connor, Dr. Craig Peters, Dr. Jim Schuck, "Plasmonic near-field antenna probing of defects in thin film photovoltaic materials", Gordon Conference, Waterville, ME, 6/9/2012

Dr. Edward Barnard\*, Dr. Brian Hardin, Dr. James Groves, Dr. Stephen Connor, Dr. Craig Peters, Dr. Jim Schuck, "Nanoscale optical and electron imaging of defects in thin-film photovoltaic materials", UEC Seminar, Berkeley, CA, 8/7/2012

Dr. Jim Schuck, Dr. Edward Barnard\*, Dr. Brian Hardin, Dr. James Groves, Dr. Stephen Connor, Dr. Craig Peters, "Plasmonic near-field antenna probing of defects in thin film photovoltaic materials", SPIE Optics and Photonics/Nano-optics, San Diego, CA, 8/14/2012

Dr. Brian Hardin\*, Dr. Edward Barnard, Dr. James Groves, Dr. Stephen Connor, Dr. Craig Peters, "It Takes A Village: Collaborating With National Labs To Accelerate R&D", Silicon Valley Leadership Group, Stanford Linear Accelerator (SLAC), Stanford, CA, 9/24/2012

Dr. Craig Peters\*, Dr. Edward Barnard, Dr. James Groves, Dr. Stephen Connor, Dr. Brian Hardin, "Probing carrier lifetimes in PV materials using subsurface two-photon microscopy", Department of Energy Review Panel for the Molecular Foundry, LBNL, 8/21/2013

**Software**

None

**Other**

None